PRODUCTION OF BORON NITRIDE

A THESIS SUBMITTED TO
THE GRADUATE SCHOOL OF NATURAL AND APPLIED SCIENCES
OF
MIDDLE EAST TECHNICAL UNIVERSITY

BY

ENGİN ÖZKOL

IN PARTIAL FULFILLMENT OF THE REQUIREMENTS
FOR
THE DEGREE OF MASTER OF SCIENCE
IN
CHEMICAL ENGINEERING

JULY 2008

Approval of the Thesis

“PRODUCTION OF BORON NITRIDE”

Submitted by **ENGİN ÖZKOL** in partial fulfillment of the requirements for the degree of **Master of Science** in **Chemical Engineering Department, Middle East Technical University** by,

Prof. Dr. Canan Özgen
Dean, Graduate School of **Natural and Applied Sciences** _______________________

Prof. Dr. Gürkan Karakaş
Head of Department, **Chemical Engineering** _______________________

Prof. Dr. H. Önder Özbelge
Supervisor, **Chemical Engineering, METU** _______________________

Assoc. Prof. Dr. İsmail Atılgan
Co-Supervisor, **Physics, METU** _______________________

Examining Committee Members:

Prof. Dr. Hayrettin Yücel (*)
ChE, METU _______________________

Prof. Dr. H. Önder Özbelge (**)
ChE, METU _______________________

Assoc. Prof. Dr. İsmail Atılgan
PHYS, METU _______________________

Assoc. Prof. Dr. Halil Kalıpçılar
ChE, METU _______________________

Assist. Prof. Dr. Barış Akaoğlu
PHYS, Gazi University _______________________

Date: _______________________

(*) Head of Examining Committee
(**) Supervisor

I hereby declare that all information in this document has been obtained and presented in accordance with academic rules and ethical conduct. I also declare that, as required by these rules and conduct, I have fully cited and referenced all material and results that are not original to this work.

Name, Last name : Engin ÖZKOL

Signature :

ABSTRACT

PRODUCTION OF BORON NITRIDE

Özkol, Engin
M.S., Department of Chemical Engineering
Supervisor: Prof. Dr. H. Önder Özbelge
Co-Supervisor: Assoc. Prof. Dr. İsmail Atılgan

July 2008, 78 pages

Boron nitride is found mainly in two crystal structures; in hexagonal structure (h-BN) which is very much like graphite and in cubic structure (c-BN) with properties very close to those of diamond. h-BN is a natural lubricant due to its layered structure. It is generally used in sliding parts of the moving elements such as rotating element beds in turbine shafts. Since c-BN is the hardest known material after diamond it is used in making hard metal covers. In addition to its possible microelectronics applications (can be used to make p-n junction), its resistance to high temperatures and its high forbidden energy gap are its superiorities over diamond.

Recent studies have shown that c-BN can be produced by Physical Vapor Deposition (PVD) and Chemical Vapor Deposition (CVD) in plasma. But these studies have failed to determine how all of the production parameters (boron and nitrogen sources,

composition of the gas used, substrate, RF power, bias voltage, substrate temperature) affect the c-BN content, mechanical stress and the deposition rate of the product with a systematic approach.

The systematic study was realized in the range of available experimental ability of the present PVD and CVD equipment and accessories. The BN films were produced in the plasma equipment for CVD using RF and MW and magnetron sputtering and were studied with the measurement and testing facilities. It is believed that with this approach it will be possible to collect enough experimental data to optimize production conditions of BN with desired mechanical and optoelectronic properties.

h-BN films were successfully deposited in both systems. It was possible to deposit c-BN films with the MW power, however they were weak in cubic content. Deposition at low pressures eliminated the hydrogen contamination of the films. High substrate temperatures led to more chemically and mechanically stable films.

Keywords: Cubic boron nitride, Plasma, Physical vapor deposition, Chemical Vapor deposition, Ion density, Bias Voltage

ÖZ

BOR NİTRÜR ÜRETİMİ

Özkol, Engin
Yüksek Lisans, Kimya Mühendisliği Bölümü
Tez Yöneticisi: Prof. Dr. H. Önder Özbelge
Ortak Tez Yöneticisi: Assoc. Prof. Dr. İsmail Atılgan

Temmuz 2008, 78 sayfa

Bor nitrür genellikle iki kristal yapıda bulunur; grafite çok benzer altıgen (h-BN) yapıda tabakalar halinde veya kübik yapıda (k-BN) elmasa çok yakın özelliklerde. h-BN lamelli yapısı sayesinde doğal bir yağlama özelliğine sahiptir. Genelde türbin şaftlarının döner eleman yatakları gibi hareketli mekanizmaların kayar parçalarında kullanılır. k-BN bilinen malzemeler içinde elmastan sonra en sert olduğundan malzeme endüstrisinde sert metal kaplamalar yapmada (elmastan daha üstün özelliklerde, metal işlemede) kullanılmaktadır. Olası mikroelektronik uygulamalarına (p-n türü katkılanabildiğinden mavi-mor bölgede algılayıcı (dedektör) veya yayınlayıcı (LED) olarak kullanılabilir) ek olarak yüksek sıcaklıklara dayanıklı olması ve yüksek yasak enerji aralığı olması elmasa olan diğer üstünlükleridir.

Son yıllarda yapılan araştırmalar k-BN'nin plazma ortamında Fiziksel Buhar Biriktirme (FBB) veya Kimyasal Buhar Biriktirme (KBB) yöntemleri ile üretilebileceğini göstermiştir. Ancak bu çalışmalar biriktirilen maddenin özelliklerine (k-BN içeriği ve mekanik gerilim) ve birikme hızına etki eden üretim parametrelerinin (kullanılan bor ve azot kaynakları, kullanılan gaz kompozisyonu, kaplanan yüzeyi oluşturan madde(taban), RF veya MW gücü, bias voltaj, taban sıcaklığı) nasıl etki ettiğini sistematik bir yaklaşımla incelememiştir.

Elde, çevre birimleriyle birlikte, kurulu bulunan hem FBB, hem de KBB düzenekleriyle (yapılabilir bazı değişiklikler ve eklerle), yukarıda sözü edilen sistematik çalışma olanaklar çerçevesinde gerçekleştirilmiştir. Başka bir deyişle hem RF hem de MW kullanan KBB ve magnetron çığlama kullanan KBB teknikleriyle büyütülen filmler, eldeki ölçüm/test düzenekleriyle çözümlenmiştir. Ancak bu yaklaşımla yeterli deneysel veri toplanarak istenen mekanik ve optoelektronik özelliklerde BN üretiminin optimum şartları elde edileceğine inanilmaktadır.

h-BN filmler, iki sistemde de başarıyla biriktirilmiştir. MW gücünün kullanılması k-BN yapıda film biriktirilmesine yol açsa da filmlerdeki kübik yapı yoğunluğu düşüktür. Düşük basınçlarda biriktirme yapmak sonucunda filmlerdeki hidrojen kirliliği yok edilmiştir. Yüksek taban sıcaklıklarında yapılan büyütmeler sonucunda ise kimyasal ve mekanik olarak daha kararlı filmler üretilmiştir.

Anahtar Sözcükler: Kübik Bor Nitrür, Plazma, Kimyasal Buhar Biriktirme, Fiziksel Buhar Biriktirme, İyon Yoğunluğu, Voltaj Farkı

To My Family

ACKNOWLEDGMENTS

First of all, I would like to thank my supervisor Prof. Dr. H. Önder Özbelge for his encouragement and inspiration that helped me in my thesis research.

I express my gratitude to Assoc. Prof. Dr. İsmail Atılgan as he is the technical backbone of this laboratory being able to execute all the present measurement and production units. He also directs the route of the research by his advices.

I am grateful to Prof. Dr. Bayram Katırcıoğlu for his advices and critics.

I greatfully appreciate Tamila Aliyeva Anutgan and Mustafa Anutgan for helping me in FTIR and profilometer analyses.

I would like to thank my friends Umut, Özlem, Mehmet, O.Kaçar, Gül, Erinç, Tahir, M.Kulakçı, M.Karaman, O.Kürüm, Atakan, E.Tekmen, Aytuğ, Metin, Botan, C.Yeniova and C.Gücüyener for their moral support during my thesis.

Lastly, I would like to express my gratitude to my family. Without their support, none of this could have been possible.

TABLE OF CONTENTS

ABSTRACT iv
ÖZ vi
DEDICATION........viii
ACKNOWLEDGMENTS ix
TABLE OF CONTENTS x
LIST OF TABLES xii
LIST OF FIGURES xiii
CHAPTERS
1. INTRODUCTION 1
  1.1. LITERATURE SURVEY ON PECVD OF BORON NITRIDE 7
  1.2. LITERATURE SURVEY ON SPUTTERING 10
  1.3. OBJECTIVE OF THE PRESENT WORK 13
2. EXPERIMENTAL 14
  2.1. EXPERIMENTAL SET-UP 14
    2.1.1. The PECVD System 14
    2.1.2. The Sputtering System 18
  2.2. CHARACTERIZATION METHODS 19
    2.2.1. FTIR Spectrometer 20
    2.2.2. UV-Vis Spectrometer 21
    2.2.3. Profilometer 22
    2.2.4. Mass Spectrometer 25
    2.2.5. X-ray Photoelectron Spectrometer (XPS) 28
  2.3. EXPERIMENTAL PROCEDURE 29
    2.3.1. Substrate Cleaning 29
    2.3.2. The PECVD Experiments 30
    2.3.3. The Sputtering Experiments 31
3. RESULTS AND DISCUSSIONS 32
  3.1. THE ANALYSES OF THE FILMS DEPOSITED IN PECVD SYSTEM 32
    3.1.1. The Analyses of The Films Deposited in The Master Unit of PECVD 32
    3.1.2. The Analyses of the Deposited Films in the Slave Unit of the PECVD 49

3.2. THE ANALYSES OF THE FILMS DEPOSITED IN SPUTTERING SYSTEM 66
4. CONCLUSIONS AND RECOMMENDATIONS 71
REFERENCES 75

LIST OF TABLES

Table 1.1. Physical properties of c-BN and h-BN[2,4] 4
Table 1.2. Comparison of the physical properties of diamond and c-BN [4] 5
Table 1.3. Literature survey on PECVD 9
Table 1.4. Literature survey on sputtering 12
Table 3.1. Deposition parameters for the master unit of the PECVD 33
Table 3.2. The wavenumbers of the peaks and corresponding structures [29-33] 34
Table 3.3. Deposition parameters of B8 and B9 experiments 35
Table 3.4. The deposition parameters of B40,41,42 and 43 experiments 36
Table 3.5. The deposition parameters of B10 and B13 experiments 38
Table 3.6. The deposition parameters of B10 and B12 experiments 40
Table 3.7. The deposition parameters of B9, B10 and B12 experiments 41
Table 3.8. The deposition parameters of B10, B14 and B15 experiments 42
Table 3.9. The forbidden band-gaps of the experiments 44
Table 3.10. The thicknesses and the deposition rates of the B7-15 experiments 45
Table 3.11. The surface concentrations and atom ratios of B7-B15 experiments 47
Table 3.12. Deposition parameters for the slave unit of the PECVD 50
Table 3.13. The deposition parameters of the B17, 23, 26 and 28 experiments 51
Table 3.14. The forbidden band-gaps of the experiments 56
Table 3.15. The thicknesses and the deposition rates of the experiments 57
Table 3.16. The observed peaks in the spectrum and the corresponding molecules . 58
Table 3.17. The surface concentrations and the atom ratios of the films 63
Table 3.18. The deposition parameters for the sputtering system 66
Table 3.19. The forbidden band-gaps of the experiments 68
Table 3.20. The thicknesses and the deposition rates of the films 69
Table 4.1. The literature limits and covered values in experiments for PECVD system 73
Table 4.2. The literature limits and covered values in experiments for sputtering system 74

LIST OF FIGURES

Figure 1.1. Three planar $sp^2-\sigma$ like bonds of boron nitride and their representation[1]. 2
Figure 1.2. p_z orbitals are perpendicular to the plane of $sp^2-\sigma$ bonds. The interaction between neighboring p_z orbitals contributes to the planar structure. 2
Figure 1.3. Six sided planar ring structure of [1]. 3
Figure 1.4. sp^2 and sp^3 bonded BN crystal structures [2]. 4
Figure 2.1. The master unit of the PECVD system [25] 16
Figure 2.2. Gas Cabinet [25] 17
Figure 2.3. Univex 450 System [24] 18
Figure 2.4. Nicolet 520 FTIR Spectrometer [25] 20
Figure 2.5. UV-Visible transmission spectroscopy system [25] 22
Figure 2.6. XP-2 Stylus Profilometer [1] 24
Figure 2.7. An example for the determination of the thickness and surface profile by the profilometer. 25
Figure 2.8. Typical HPR30 work station arrangement [26] 27
Figure 2.9. HPR30 vacuum schematic [26] 28
Figure 3.1 A typical IR spectra observed in experiments and the deconvolution of the peaks (B9 experiment) 34
Figure 3.2 The effect of pressure on IR spectrum of B8 and B9 experiments 35
Figure 3.3. The spectrum of B36 experiment, which was carried out at room temperature, at the deposition day (blue) and 3 days after the deposition (red) 36
Figure 3.4. The spectrum of B36 experiment, which was carried out at 125 °C, at the deposition day (blue) and 3 days after the deposition (red) 37
Figure 3.5. The spectrum of B36 experiment, which was carried out at 250 °C, at the deposition day (blue) and 3 days after the deposition (red) 37
Figure 3.6. The spectrum of B36 experiment, which was carried out at 350 °C, at the deposition day (blue) and 3 days after the deposition (red) 38
Figure 3.7. The effect of applied power on IR spectrum of B10 and B13 experiments 39

Figure 3.8. The effect of applied bias voltage on the substrates on IR spectrum of B10 and B12 experiments 40
Figure 3.9. The effect of N_2/B_2H_6 ratio on IR spectrum of B9, B10 and B11 experiments 41
Figure 3.10. The effect of argon addition to the process gases on IR spectrum of B10, B14 and B15 experiments 43
Figure 3.11. A typical XPS spectra (B10 experiment) 46
Figure 3.12. The IR spectra of the B17 experiment 51
Figure 3.13. The IR spectra of the B23 experiment 52
Figure 3.14. The IR spectra of the B26 experiment 52
Figure 3.15. The IR spectra of the B28 experiment 53
Figure 3.16. The spectrum of films deposited at different N_2/B_2H_6 gas ratios 54
Figure 3.17. The spectrum of B22 experiment at the deposition day (blue) and 7 months after the deposition (red) 54
Figure 3.18. The spectrum of B36 experiment at the deposition day (blue) and 15 days after the deposition (red) 55
Figure 3.19. The mass spectra observed when a string of hair was placed on the gasket of the cover of the plasma chamber 59
Figure 3.20. The mass spectra of B19 experiment before the process gases were given to the chamber (high partial pressure of nitrogen, peak located at 28 amu) 59
Figure 3.21. The mass spectra of B26 experiment before the process gases were given to the chamber (moderate partial pressure of nitrogen, peak located at 28 amu) 60
Figure 3.22. The mass spectra of B35 experiment before the process gases were given to the chamber (low partial pressure of nitrogen, peak located at 28 amu) 60
Figure 3.23. The mass spectra of B39 experiment before the process gases were given to the chamber (no partial pressure of nitrogen, peak located at 28 amu) 61
Figure 3.24. The mass spectra of B33 experiment after the process gases were given to the chamber 62
Figure 3.25. The mass spectra of B33 experiment after the plasma formation in the chamber 62

Figure 3.26. The wide mass spectra of B33 experiment after the plasma formation in the chamber 63
Figure 3.27. The IR spectrum of B46 and B50 experiments 67
Figure 3.28. The UV-Vis spectra of the B49 experiment 68

CHAPTER 1

INTRODUCTION

Boron nitride (BN) is an inorganic material that is a candidate to have a wide application area in industry due to the similar crystal structures and phase changes as carbon, high thermal shock resistance, high thermal conductivity, high dielectric constant, chemical stability, and lubricating property [1].

Boron can form 3 covalent bonds by sp^2 hybridization $(1s^2 2s^1 2p_x^1 2p_y^1)$, although the boron atom in its normal electronic configuration has only one half filled orbital ($1s^2 2s^2 2p^1$). Since nitrogen has 3 half filled orbitals ($1s^2 2s^2 2p^3$), it normally forms three covalent bonds. So, both for boron and nitrogen, 3 equivalent orbitals may be obtained by combining one 2s-orbital with two 2p-orbitals (planar $2p_x$ and $2p_y$) as three sp^2 hybrid orbitals.

Three planar sp^2-like σ bonds are formed around each of the components as seen in Figure 1.1. Nitrogen has greater nuclear charge when compared to boron, so atomic orbitals on the nitrogen are located relatively lower in potential energy. Due to that, in these hetero-nuclear diatomic σ bonds, electrons are expected to be concentrated rather towards the nitrogen atom.

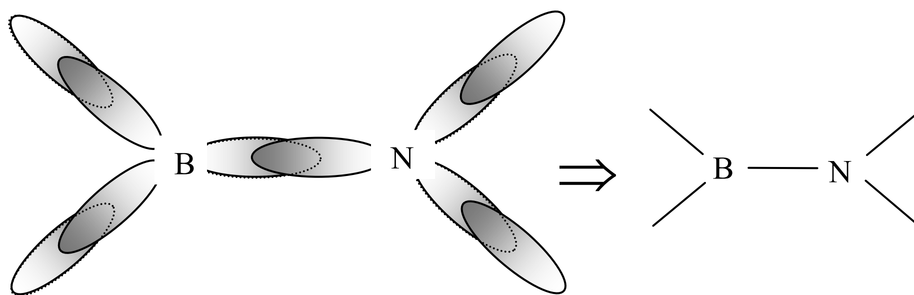

Figure 1.1. Three planar $sp^2-\sigma$ like bonds of boron nitride and their representation[1].

During the formation of above described three planar sp^2-like σ bonds around both B and N atoms, an unhybridized free p_z atomic orbital remains on each component, which are perpendicular to the plane of the three sp^2 orbitals. As mentioned earlier, the nitrogen orbital $(p_z)_N$ is lying lower in potential energy than that of the boron $(p_z)_B$. Consequently, $(p_z)_N$ is expected to be occupied by two electrons and $(p_z)_B$ remains empty (it is assumed here that one of the 2s^2 electrons of nitrogen atom participates in sp^2 bonding, the other is excited to $(p_z)_N$ orbital). Moreover, the lobes of $(p_z)_B$ and $(p_z)_N$ above and below the sp^2 bonds should be symmetrically cut by the plane of sp^2 bonds as seen in Figure 1.2[1].

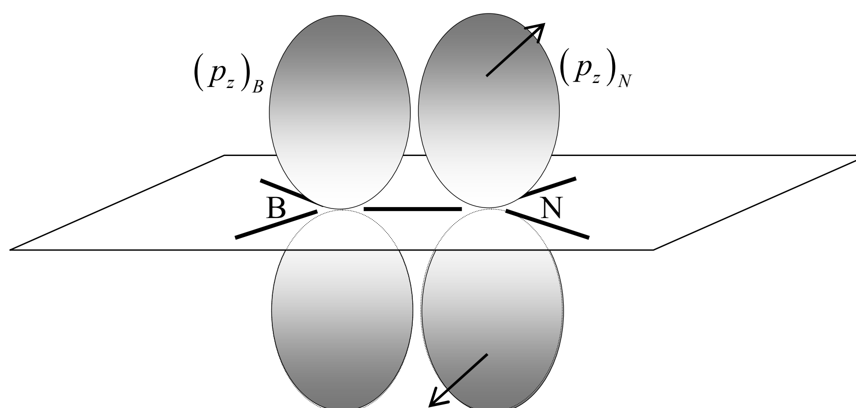

Figure 1.2. p_z orbitals are perpendicular to the plane of $sp^2-\sigma$ bonds. The interaction between neighboring p_z orbitals contributes to the planar structure.

In boron-nitrogen combination, each component atom of one sort has three planar trigonal $sp^2-\sigma$ bonds 120º apart to three atoms of second sort. The configuration may easily lead to six sided planar ring structure [1] as seen in Figure 1.3.

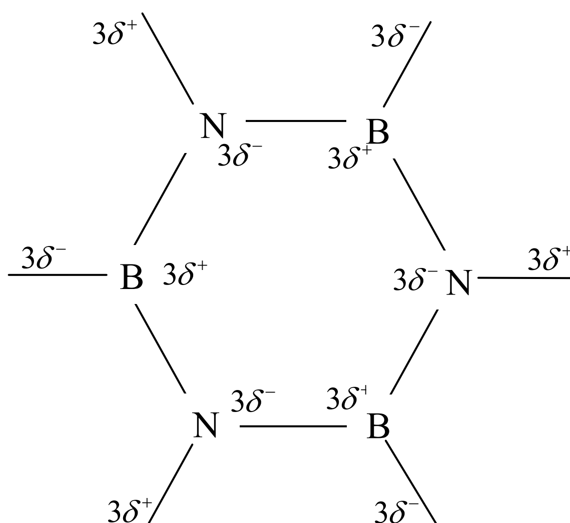

Figure 1.3. Six sided planar ring structure of [1].

The above described hexagonal structure has ability to be arranged into a three $sp^2-\sigma$ like coordinated hexagonal 2-dimensional infinite layers. These layers composed of six-fold B_3N_3 rings of a giant planar molecule are held together by weak van der Waals or dipolar interaction. As depicted in Figure 1.4, these hexagons are packed directly on top of each other where a boron atom in one layer remains closest to each corresponding nitrogen atom in the neighboring layers with ABAB… sequence of planes[1].

In cubic BN arrangement, the components boron and nitrogen supply 8 valence electrons which are hybridized from the linear combination of $2s^1 2p_x^1 2p_y^1 2p_z^1$ atomic orbitals of both B and N atoms into 4 sp^3 identical orbitals equivalently located in space around each component; these hybrid orbitals from one component form σ-like tetrahedral bonds with the four neighboring second component[1] as shown in Figure 1.4.

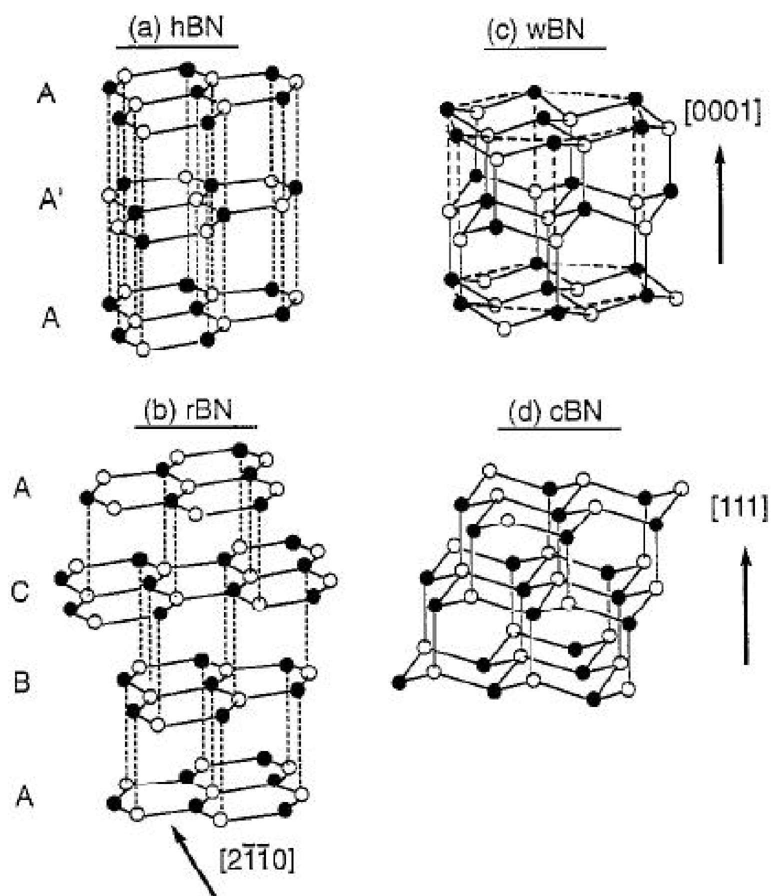

Figure 1.4. sp^2 and sp^3 bonded BN crystal structures [2]

BN, have sp^2 and sp^3 bonded phases, which are compared to carbon. c-BN is similar to diamond in many ways and also known as 'better diamond', whereas h-BN shows the same characteristics as graphite and also known as 'white graphite'. The physical properties of c-BN and h-BN is given in Table 1.1.

Table 1.1. Physical properties of c-BN and h-BN[2-4]

Properties	c-BN	h-BN
Density (g/cm^3)	3.48	2.27
Thermal Conductivity, 25 ºC (W/m.K)	1300	55
Dielectric Constant	5.8	4.2
Melting Temperature (ºC)	2973	2700
Oxidation Temperature (ºC)	1200	980

h-BN is a natural lubricant due to its layered property. It can be used both at high and low temperatures. Moreover it has low dielectric constant, high electrical resistance, excellent thermal shock resistance and it is chemically inert. So it can be used as lubricant in situations where the electrical conductivity or chemical reactivity of graphite might be problematic. h-BN is mainly used in paint, dental cement, sliding parts of moving mechanisms, rotating element beds in turbine shafts, diesel turbo-charges [3].

c-BN is the second hardest material after diamond known up to now. The oxidation temperature of c-BN is 1200 ºC, which is much higher than that of diamond (600 ºC). Moreover, while diamond is reactive to ferrous materials, c-BN acts as an inert. Additionally, while diamond cannot be n-type doped since no potential donor atom which will yield a shallow enough energy level in the gap to be sufficiently ionized at room temperature is found up to now, c-BN can be doped both p- and n- type. So, it is possible to produce the p-n junction which is the fundamental element of the electronic circuits. Therefore, it could be used as a violet-blue region light detector and light emitting diode (LED). c-BN has a band gap of 6.2-6.6 eV that is higher then diamond (5.51 eV). So it could be used at higher temperatures for opto-electronic applications. The comparison of the physical properties of diamond and c-BN is given in Table 1.2.

Table 1.2 Comparison of the physical properties of diamond and c-BN [5]

Properties	Diamond	c-BN
Density(g/cm^3)	3.51	3.48
Hardness(GPa)	100	75
Elastic Modulus(GPa)	1140	850
Thermal Conductivity (W/cmK)	20	13
Oxidation Temperature (ºC)	600	1200
Refractive Index	2.417	2.117
Band Gap (eV)	5.51	6.2-6.6
Reactivity to Ferrous Materials	High	Inert

For the deposition of c-BN thin films, chemical vapor deposition (CVD) and physical vapor deposition (PVD) techniques are used [5]. Electron cyclotron resonance plasma CVD and plasma enhanced CVD (PECVD) could be given as an example of CVD routes, whereas magnetron sputtering and ion beam assisted deposition could be given as examples of PVD methods. CVD is advantageous over PVD in terms of low cost, purity, 3 dimensional and wide area coating.

Plasma is a necessity in many c-BN deposition processes. Energy can be supplied (thermal energy by increasing the temperature or electromagnetic energy by radio frequency (RF) or microwave (MW)) to a gas, the atoms and compounds are ionized gradually and plasma is formed from the positively charged ions, electrons and uncharged, deionized atoms.

While producing thin films in laboratory, generally glow discharge is formed under relatively low pressure with radio frequency (RF) or microwave (MW) generated electric field. In such a plasma, the following phenomena may take place [3]:

- In high frequency electric field, gases ionize into electrons and ions. The electrons with their so small masses accelerated to 5000 K (necessary electron temperature which corresponds to nearly 1 eV for the formation of a glow discharge at vacuum) or higher energy levels immediately.
- The heavy ions which have more inertia than electrons cannot respond to the fast changes in the electric field. Therefore, their temperature and the temperature of the plasma remain lower than the electron temperature.
- Electrons, that have high energies, collide with gas molecules to form reactive radicals and end up with the the chemical reactions.

Sputtering is one of the most commonly used techniques in PVD for depositing thin films. It is simply the ejection of the atoms from the target due to the high energy ion bombardment of the energetic neutral molecules or ions [6]. In other words, it could be considered as a cleaning method due to the ejection of the atoms from the surface by the created collisions [7]. These ejected atoms from the surface are deposited on the substrates.

1.1. LITERATURE SURVEY ON PECVD OF BORON NITRIDE

Carreno et al. [8] deposited boron nitride (BN) thin films on silicon substrates using diborane (B_2H_6) and nitrogen (N_2) as source gases. The effects of temperature, RF power and N_2/B_2H_6 ratio on the structure of the films were investigated while keeping the pressure lower than 1 Torr. Hexagonal BN (h-BN) films were obtained in all experiments. Temperature seemed to have no effect on the structure on the films while at high RF powers and gas ratios, the hexagonal crystallinity of the films got poorer.

Abdellaoui et al. [9] deposited h-BN in a PECVD reactor at 320 °C, 120 mTorr, and MW plasma power of 500W by using borane dimethylamine ($BH_3NH(CH_3)_2$) as the boron source. Argon gas was used as the carrier gas of boron source and N_2 was used as the nitrogen source. Silicon, quartz and pyrex substrates were used for structural and optical analyses. An optical gap of 3.6 eV was determined.

Mekki et al. [10] investigated the structures of the deposited BN films by using B_2H_6-H_2-NH_3, B_2H_6-N_2, and B_2H_6-N_2-Ar gas mixtures. The experiments were carried out at 300 °C and 4 $mW.\mu m^{-2}$. The obtained structure was hexagonal, as seen in FTIR and Raman spectrum.

Rossi et al. [11] used BCl_3-N_2-H_2-Ar gas mixture to deposit BN films at 300 °C, 500W, and 53 Pa on silicon substrates. The films contained maximum 15-20 % cubic BN (c-BN) while the rest was h-BN.

Vilcarromero et al. [12] investigated the flow rates of the gases in the B_2H_6-N_2-H_2 mixture on the structure of the deposited BN films. At high B_2H_6 flow rates (therefore low N_2/B_2H_6 ratio) well-oriented hexagonal crystallites were obtained. On the other hand, at low B_2H_6 flow rates (therefore high N_2/B_2H_6 ratio) the cubic onset was obtained.

Soltani et al. [13] deposited BN films in microwave PECVD system, using borane dimethylamine as the boron precursor. To promote the cubic phase formation, negative bias voltage in the range of 30-200 V was applied to the substrates. The applied RF power was in the range of 7-25 W, whereas the applied MW power was in the range of 200-500W. Temperature was kept constant at 300 °C. At -160V of bias voltage, the deposited films have a fraction of c-BN more than 95%. Moreover, the films deposited in this system showed no delamination after 6 months.

Deb et al. [14] studied PECVD of BN in a temperature range of 623-773 K and a RF power range of 200-250 W, using borane-ammonia and nitrogen as the precursor gases. The films were deposited on silicon and quartz substrates in order to investigate the structural and optical properties. The film deposited at 623 K, 0.5 mbar, and 200W contained about 50 % c-BN and had a bandgap of 6 eV.

Chan et al. [15] used fluorine chemistry for the deposition of BN films in MW power generated PECVD. The gas mixture was He-Ar-N_2-BF_3-H_2 while 1400W of MW power, 1.6 mTorr, 900 °C, -40V substrate bias were the medium conditions. The deposited film had about 85 % of cubic phase with a thickness of 1.1 μm. It was shown that with fluorine chemistry and the reacting gas mixture, low stressed films could be produced, which means thicker coatings.

Battiston et al. [16] used borane dimethylamine as the boron source in the plasma power optimization for the maximum c-BN content. The deposition is carried out in Ar-N_2 atmosphere at 80-90 Pa and varying temperature of 280-550 °C. It was determined that powers up to 330 W, only h-BN forms with no temperature dependency. It was shown that after deposition of h-BN containing films, annealing at 1000 °C in nitrogen atmosphere, at normal pressure led to a complete transformation into cubic phase and this temperature is the threshold value for complete transformation.

A summary of the literature survey on PECVD of BN is given in Table 1.3.

Table 1.3. Literature survey on PECVD

Reference	Substrate	Substrate Temperature (°C)	Power (W)	Precursors	Pressure	Bias Voltage (V)	Maximum c-BN (%)
Battiston et al. [16]	Si	280-550	330 (RF)	$BH_3NH(CH_3)_2$- Ar- N_2	80-90 Pa	-	-
Chan et al. [15]	Si	900	1400 (MW)	He-Ar-N_2-BF_3-H_2	1.6 mTorr	-40	85
Deb et al. [14]	Si, Quartz	350	200 (RF)	BH_3NH_3-N_2	0.5 mbar	-	50
Soltani et al. [13]	Si	300	7-25 (RF) 200-500 (MW)	$BH_3NH(CH_3)_2$- Ar- N_2	0.06-0.2 torr	-160	95
Vilcarromero et al. [12]	-	-	-	B_2H_6-N_2-H_2	-	-	-
Rossi et al. [11]	Si	300	500 (RF)	BCl_3-N_2-H_2-Ar	53 Pa	-140	20
Mekki et al. [10]	Ni-Cr coated Si, Si, Corning glass	300	-	B_2H_6-H_2-NH_3, B_2H_6-N_2, B_2H_6-N_2-Ar	-	-	-
Abdellaoui et al. [9]	Si, Quartz	320	500 (RF)	$BH_3NH(CH_3)_2$	120 mTorr	-	-
Carreno et al. [8]	Si	200-500	-	B_2H_6-N_2	1 Torr	-	-

1.2. LITERATURE SURVEY ON SPUTTERING

Ulrich et al. [17] deposited high-purity c-BN films by RF magnetron sputtering of a h-BN target combined with argon ion bombardment at 300W of RF power. The residual stress on the films were investigated and to reduce this stress, six different mechanisms were suggested; (1) Deposition at high substrate temperatures, (2) post-annealing, (3) post-ion implantation, (4) addition of carbon or silicon to the alloy, (5) multilayer consept, (6) optimization of the deposition parameters.

Zhou et al. [18] used nickel substrates instead of silicon for boron nitride deposition by magnetron sputtering. The deposition was carried out in an Ar/N_2 gas medium at a pressure of 10-15 mTorr. At lower RF power such as 60-80 W, a negative bias voltage in the range of 150-300 V was applied to the substrates, which were heated up to 600 °C, led to about 90% c-BN fraction in the films. The experiment showed that nickel may also be a promising substrate material for the preparation of high quality and well adherent c-BN films.

Jiang et al. [19] investigated the effect of bias voltage during the deposition in an RF magnetron sputtering system. The experiment was carried out at 250 °C, 330 W of RF power, 1.5 x 10^{-3} mbar, and Ar/N_2 medium [9:1]. The nucleation of the c-BN was done under -75 V of substrate bias, then it was reduced to -50 V for growth. The films compared to the one-step growth, showed lower mechanical stress and more purity with respect to c-BN fraction.

Ding et al. [20] investigated the effects of substrate bias voltage, temperature, RF power, and Ar/N_2 gas ratio on the structure of the films. A threshold value of -150 V was determined for the cubic phase formation. A relatively higher substrate temperature favored the c-BN formation. Increase in the power led to increase in the deposition rate but not the cubic phase content. The optimum gas ratio was determined to be 5, to have the highest c-BN content of 75 % at 800 W, 400 °C, and -150 V.

Kotake et al. [21] studied the dependence of the phase selection of BN on the lattice parameter and the crystal structure of the substrate. BN thin film was prepared by RF sputtering method on Cu, Ni–Cu solid solution alloy and silicon substrates. The ratio of c-BN phase on Cu substrate was found to be three times larger than that on $Ni_{0.8}$–$Cu_{0.2}$ alloy and was minimum on Si. The results implied that the smaller the lattice-mismatch, the more stable the c-BN thin films.

Le et al. [22] investigated the effect of the substrate temperature on RF magnetron sputtering of BN. It was shown that there is no threshold limit for temperature. For a substrate bias of -200 V, c-BN growth was obtained even close to room temperature, when the N_2 content in the N_2/Ar working gas exceeds 7%. The better adherence (or longer lifetime) of cBN-films deposited at low substrate temperatures may be ascribed to thicker h-BN sublayers than those for higher temperature depositions. On the other hand, the fraction of c-BN was found to be increased while increasing temperature.

Caicedo et al. [23] investigated the cubic phase formation threshold values for both DC and RF bias voltages. It was seen that at the bias below -150 V DC biased and -90 V RF biased, only h-BN was formed. The layered BN film was also determined by atomic force microscopy (AFM). The first layer deposited was a-BN with a thickness of 100 nm, the second layer was h-BN with a tickness of 50 nm and after this film of 150 nm thick, c-BN started to nucleate and grow as the third layer.

A summary of the literature survey on sputtering is tabulated in Table 1.4.

Table 1.4. Literature survey on sputtering

Reference	Magnetron Power (W)	Substrate	Substrate Temperature (ºC)	Gas Mixture	Pressure	Bias Voltage (V)	Maximum c-BN (%)
Caicedo et al. [23]	120	Si	300	Ar:N [19:1]	4×10^{-2} mbar	-150	85
Le et al. [22]	400	Si	200	$Ar:N_2$ [9:1]	2.6×10^{-3} mbar	-200	90
Kotake et al. [21]	180	Cu-Ni alloy, S	27-727	$Ar:N_2$ [7:3]	2×10^{-4} Pa	-200	-
Ding et al. [20]	800	Si	400	$Ar:N_2$ [5:1]	3×10^{-3} Torr	-150	75
Jiang et al. [19]	330	Si	250	$Ar:N_2$ [9:1]	$1.3\text{-}.15 \times 10^{-3}$ mbar	-50 to -80	96
Zhou etal. [18]	60-80	Ni	400-500	$Ar:N_2$ [5:1]	10-15 mTorr	-150 to -300	90
Ulrich et al. [17]	300	Si	500-600	Ar	0.08 Pa	-	-

1.3. OBJECTIVE OF THE PRESENT WORK

Recent studies showed that c-BN could be deposited in plasma medium by chemical vapor deposition (CVD) and physical vapor deposition (PVD) techniques. However, a systematical approach to understand the effects of the deposition parameters, such as the boron and nitrogen sources, gas compositions, RF and MW powers, substrate bias and temperature, on the deposited films' properties such as c-BN fraction and stress, and on the deposition rate had not been made yet. In every single work, different parameters were investigated, therefore it could not be possible to integrate those studies into industrial production. In that manner, a systematic study will be an important contribution to possible optimization of the experimental parameters for the commercial production of BN.

CHAPTER 2

EXPERIMENTAL

2.1. EXPERIMENTAL SET-UP

2.1.1. The PECVD System

The PECVD system consists of two different reaction (or etching) chambers. The master unit is an RF generated plasma decomposition system, whereas in the slave unit, plasma can be generated by either RF or MW or both (according to the requirements). Both units are controlled by the same main frame. The master unit is shown in Figure 2.1.

The master unit is a capacitative coupling type reactor, which has an electrode diameter of 24 cm. The distance between the electrodes are 40 mm. RF power is applied to the upper electrode. The process gases are introduced to the chamber from the middle of the upper electrode. Substrates are placed on the lower electrode, which can be heated up to 400 °C. Also, bias voltage is applied to the lower electrode. To avoid the overheating of the system cooling water lines are available where needed.

The slave unit is also a capacitative coupling type reactor, but the main differences are the MW power generator and magnets placed for electron cyclotron resonance (ECR) on the upper electrode. The MW generator gives 800 W to the system from the top of the reactor. The lower electrode has a diameter of 18 cm. RF power is

applied to the lower electrode. The process gases are introduced from the edges of the upper electrode. Substrates are again placed on the lower electrode, where the self bias voltage is applied. However, the lower electrode of the slave unit cannot be heated. The most outstanding advantage of the slave unit is the mass spectrometer connection to the chamber.

The RF signal of 13.56 MHz is supplied by RF generator with maximum power of 300W [24]. The RF power introduced to the electrodes is adjusted manually by the matching unit, which minimizes the reflected power. The MW generator produces a constant power of 800 W under continuous or pulsed operation. Pulse length can be adjusted from 0.1 to 5 seconds.

Since some of the process gases are flammable and toxic, it is a safety problem to exhaust them into air. To solve this problem, a combustion furnace, which operates at 800 °C, was placed between the reaction chambers and the pump. According to the gases used, some dust such as boron or silicon dust might be produced in the furnace. A dust filter avoids these solid particles to reach the pump, so protects the pump. During this process, the gas lines are continuously purged with N_2.

Most of the process gases such as boron trichloride (BCl_3), diborane (B_2H_6) and silane (SiH_4) are not only reactive but also toxic and flammable. Therefore these gases are placed into a cabinet which is donated with an aspirator system to change the air within the cabinet for each minute [24]. The gas handling system is shown in Figure 2.2.

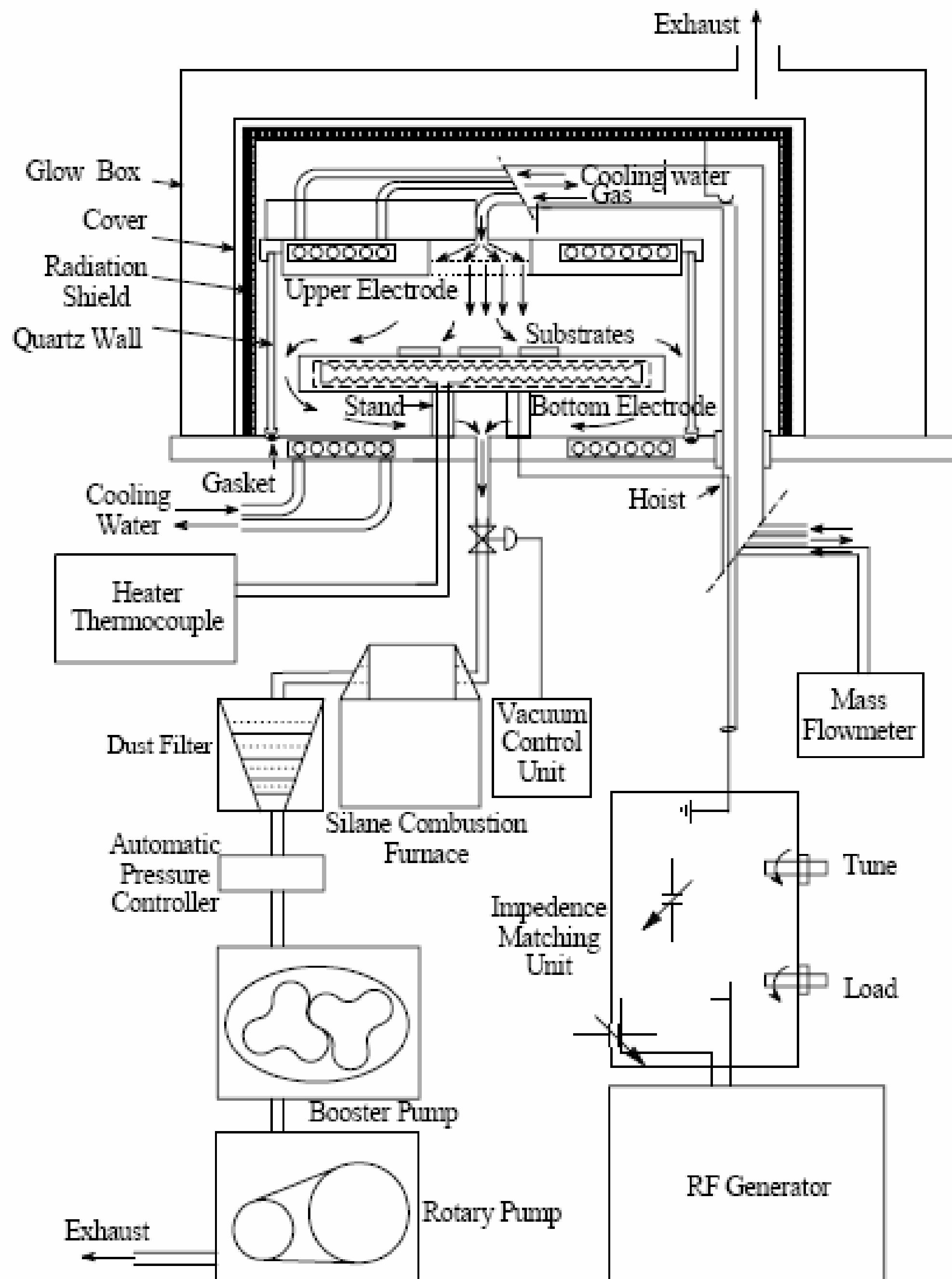

Figure 2.1. The master unit of the PECVD system [25]

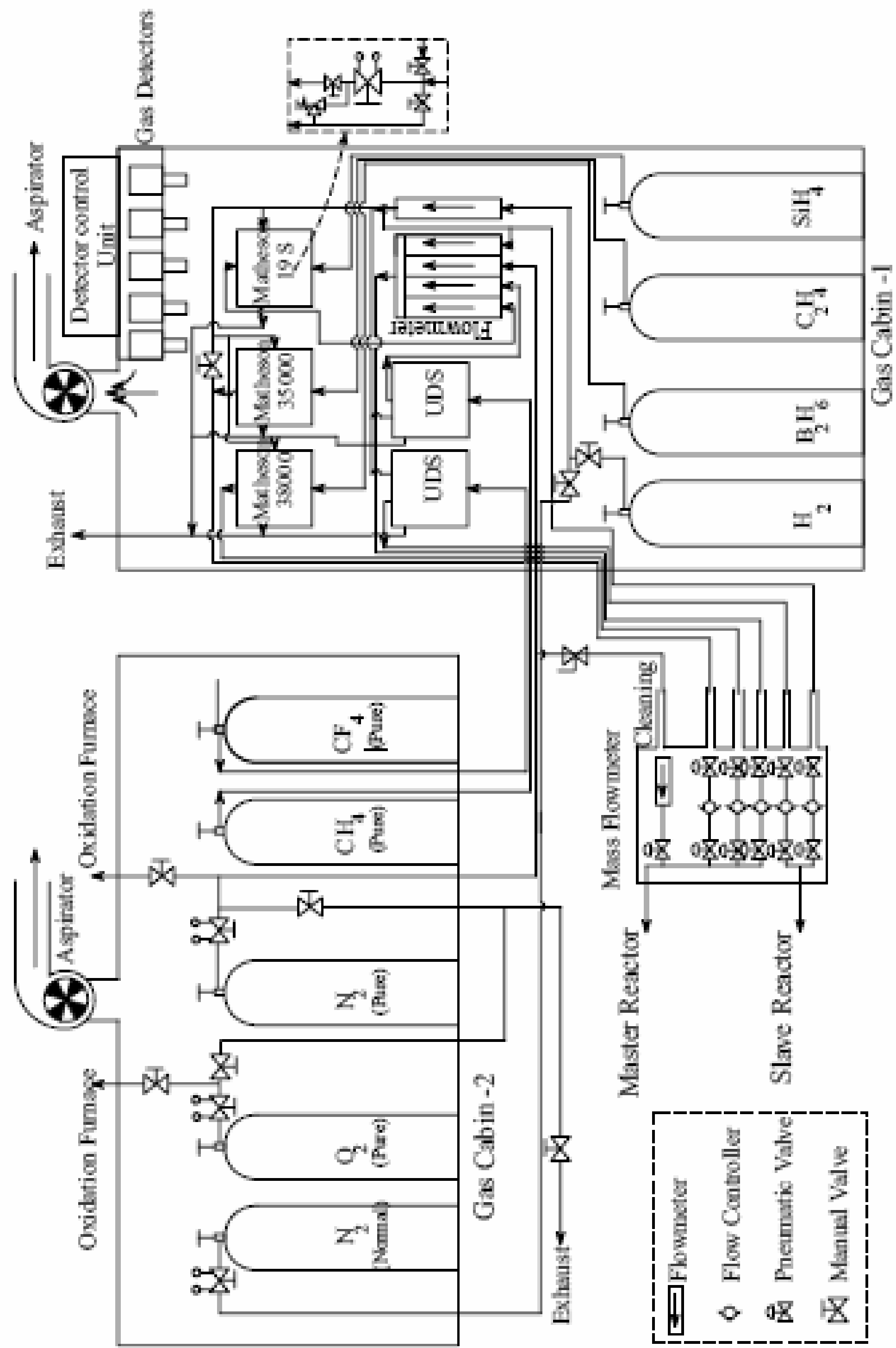

Figure 2.2. Gas Cabinet [25]

2.1.2. The Sputtering System

The Univex 450 system, shown in Figure 2.3, is a versatile vacuum coater for thermal evaporation, electron beam evaporation, glow discharge, and sputtering processes. The whole system is made of stainless steel to minimize leakage. Also, a hoist system is used to lift up the heavy chamber cover. The system consists of several parts such as sample holder, pumps, heater, and thickness monitor.

The sample holder can be rotated in a speed range of 0 to 150 rpm which enhances the coating uniformity. The sample temperature can be heated up to 400 °C by the help of infrared heater.

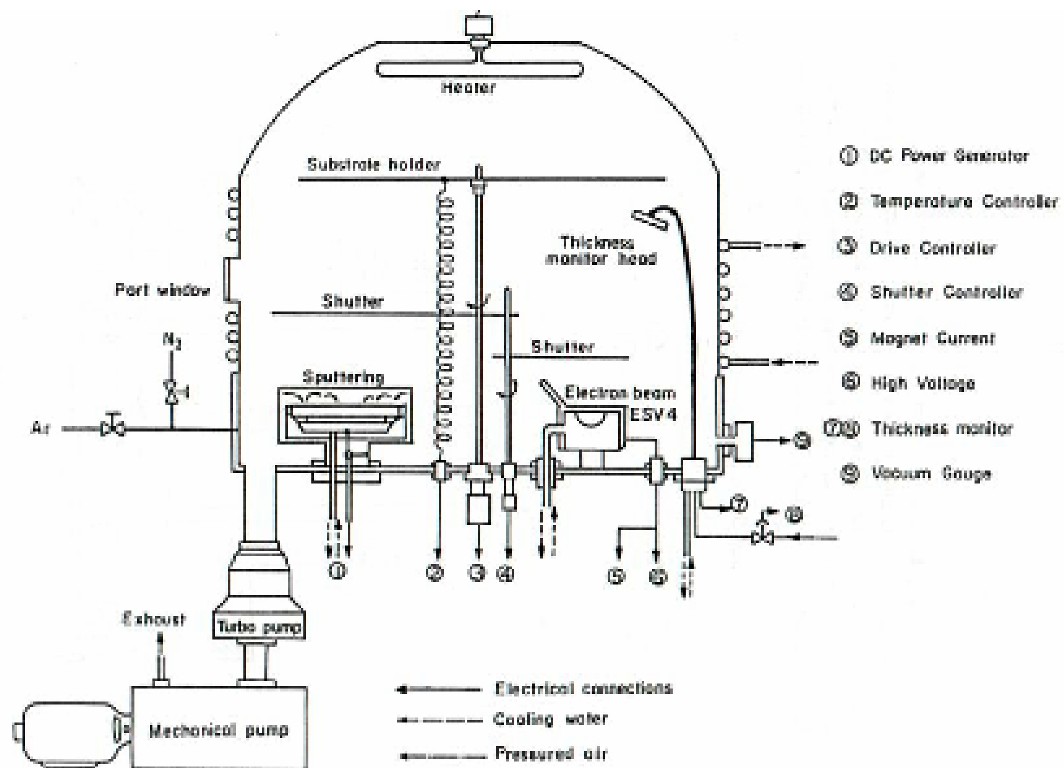

Figure 2.3. Univex 450 System [24]

Pumping system is a series connection of a mechanical and a turbomolecular pumps. This series connection leads to the elimination of the pumping sequence control by starting the pumps together. The mechanical pump is used to reduce the pressure to 0.1 torr and then turbomolecular pump starts to operate. It can reduce the pressure up to 10^{-7} torr. The vacuum level is monitored by two gauges; pirani (up to 10^{-3} torr) and ion (for higher levels) gauges.

The thickness is controlled and monitored by XTC thickness monitor and control unit. The thickness of the film is measured by the resonant frequency of the piezoelectric crystal. However, the deposition rate on the crystal and on the substrates may differ; therefore a correction factor should be used for the actual thickness.

The sputtering unit of this system is a planar magnetron sputtering system driven by power sources of DC (1500 W) and RF (1200 W). The cathode is surrounded by the anode like annulus geometry so that the ions will be directed toward the cathode with an oblique (>45°) angle. The circular magnet is placed behind the target to minimize the electron loss. Due to the high power dissipation, cooling of the target is so important for the continuous operation which is done by cooling water in the system.

2.2. CHARACTERIZATION METHODS

For the characterization of the deposited thin films, infra-red (FTIR), ultra-violet visible region spectroscopy (UV-Vis), electron spectroscopy for chemical analysis (ESCA) or in other words x-ray photoelectron spectroscopy (XPS), and mass spectrometer (MS) and profilometer were used.

2.2.1. FTIR Spectrometer

Nicolet 520 FTIR spectrometer was used for the determination of the bonding structures of the deposited thin films in the necessary infra-red range. For these measurements, double side polished silicon substrates, which are transparent in IR region, were used.

Nicolet 520 FTIR Spectrometer mainly consists of four parts, which are an air pump, an air drying unit, FTIR spectrometer and a computer as seen in Figure 2.4.

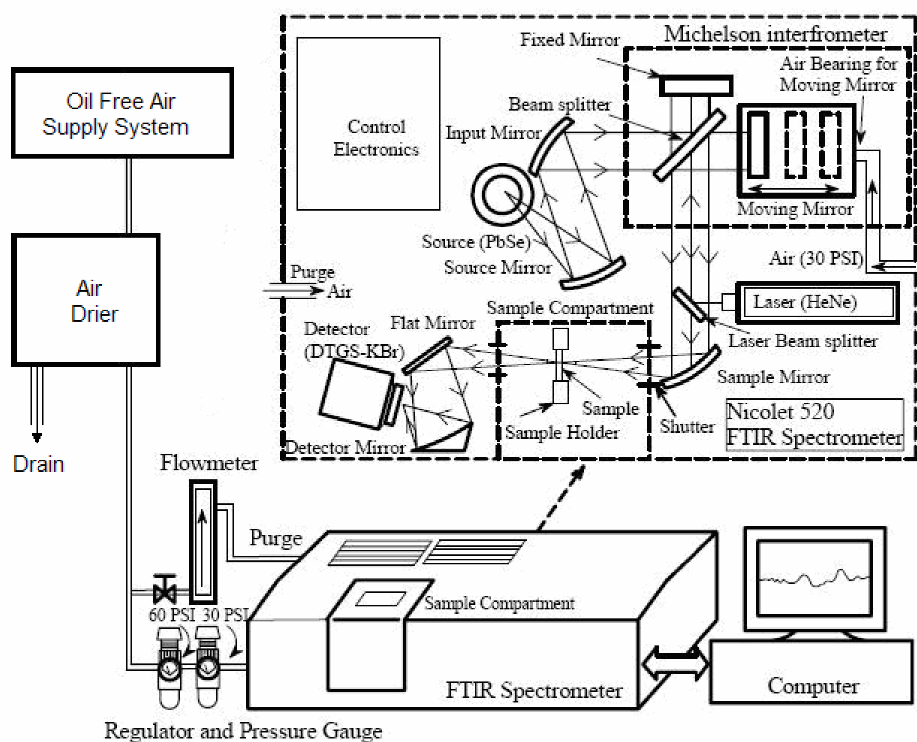

Figure 2.4. Nicolet 520 FTIR Spectrometer [25]

The air pump and the air drying unit are used to purge the system to avoid volatile material contamination such as water vapor and CO_2.

The spectrometer consists of three main components: A source (PbSe), a Michelson interferometer and a detector (DTGS-KBr). The Michelson interferometer, which consists of a beamsplitter, a fixed mirror and a moving mirror, preserves both frequency and intensity information and replaces the conventional monochromator [25].

The computer is used for the control of the system and, data collection and processing. However, for the processing of the data, a more complicated software program PEAK FIT was used.

2.2.2. UV-Vis Spectrometer

The energy band gap, refractive index, thickness and the absorption coefficient of the films can be determined by the UV-Vis transmission spectroscopy. For this purpose, films deposited on quartz substrates were used.

The measurements are made by Perkin Elmer Lambda 2S double beam spectrometer. The system consists of a monochromator with concave holographic grating with 1053 lines/mm for a wavelength range of 200-1100 nm, two photo-diode detectors and a computer. Deuterium and Tungsten-halogen lamps are the radiation sources, and the transmittance is detected by photo-diode detectors [25]. The schema of the system is given in Figure 2.5.

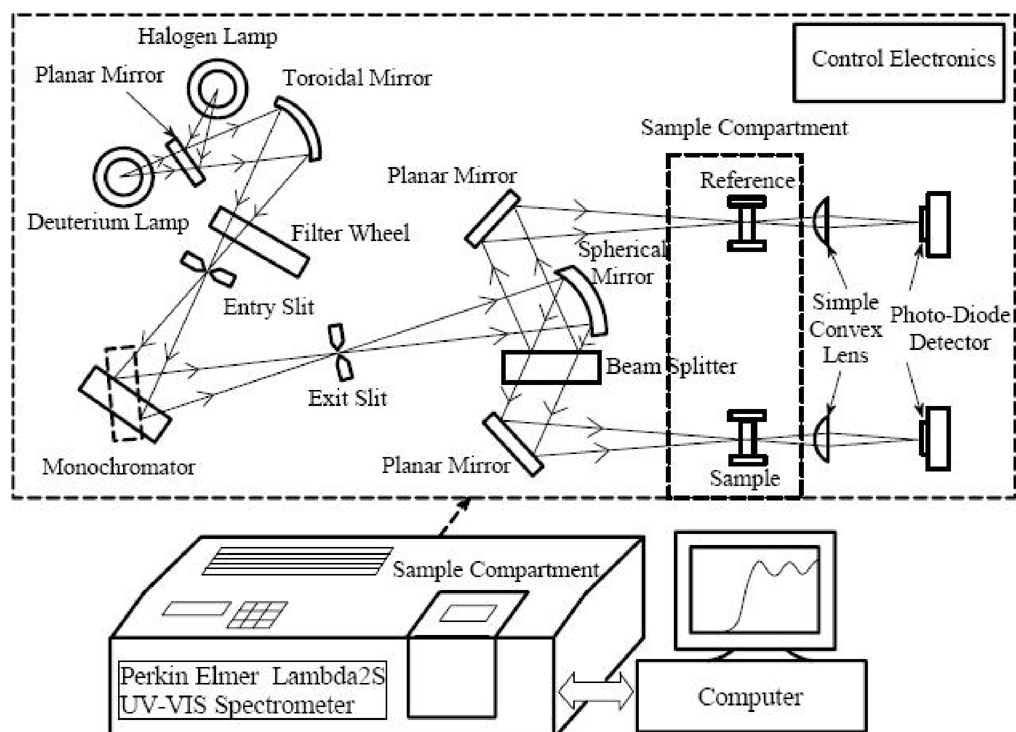

Figure 2.5. UV-Visible transmission spectroscopy system [25]

2.2.3. Profilometer

For determination of the thickness of the films and the deposition rates AMBIOS XP-2 stylus profilometer was used.

The profilometer has a tip radius of 2.0 microns which has detection limits of 100 nm horizontally and 6.2 nm vertically to obtain surface profile of the films. The applied force to the stylus is in the range of 0.05-10 mg. To keep this force constant through a rough surface, the force coil creates a suitable moment on the frictionless pivot. For the determination of the tip height, a red laser light is reflected from the mirror-like back of the tip holder and aimed to the split photo detector (SPD). The subtraction of the signal intensities received by the subdetectors of the SPD gives the height of the

cavities. For instance, when the tip holder is horizontal (zero altitude) the laser light is equally shared by both sub-detectors of the SPD. Then, the signal intensities of both subdetectors are subtracted from each other and zero altitude is verified. On the other hand, when the tip holder is passing through a cavity, the laser light would be rather projected more on the lower or upper sub-detector. In this case, the subtraction of the signal intensities does not give zero and the resultant signal is amplified for a precise height determination. The result is loaded to the computer screen as the two dimensional surface profile of the sample [1]. The schematic diagram of the system is given in Figure 2.6.

For the thickness determination, shadow masks are placed on the substrates to form grooves on the films as shown in Figure 2.7. The assumption made for thickness calculation is that there is no deposition under the masks. An average thickness is calculated by taking several tip paths. After the thickness is obtained, by dividing it to the deposition time an average deposition rate is determined.

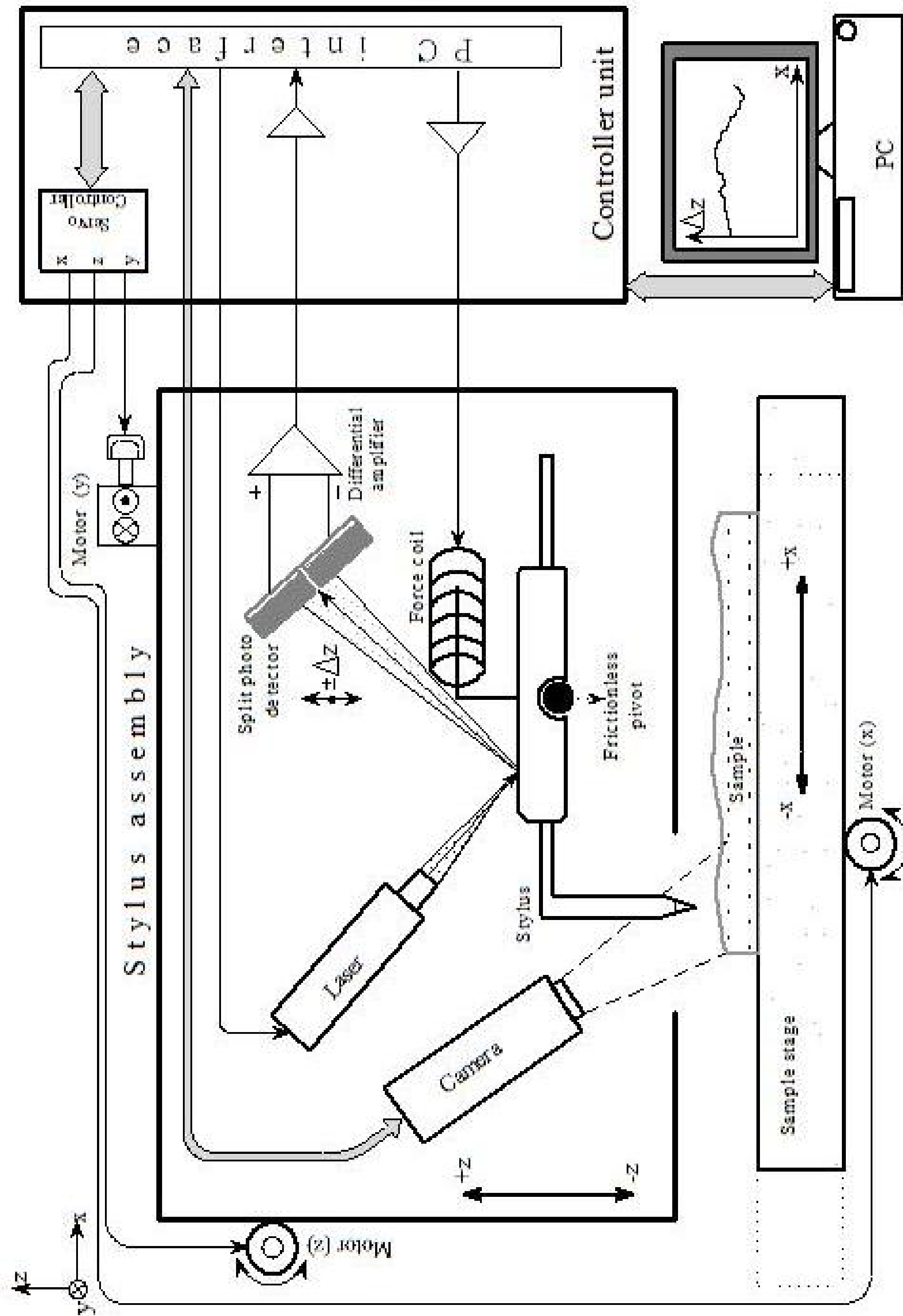

Figure 2.6. XP-2 Stylus Profilometer [1]

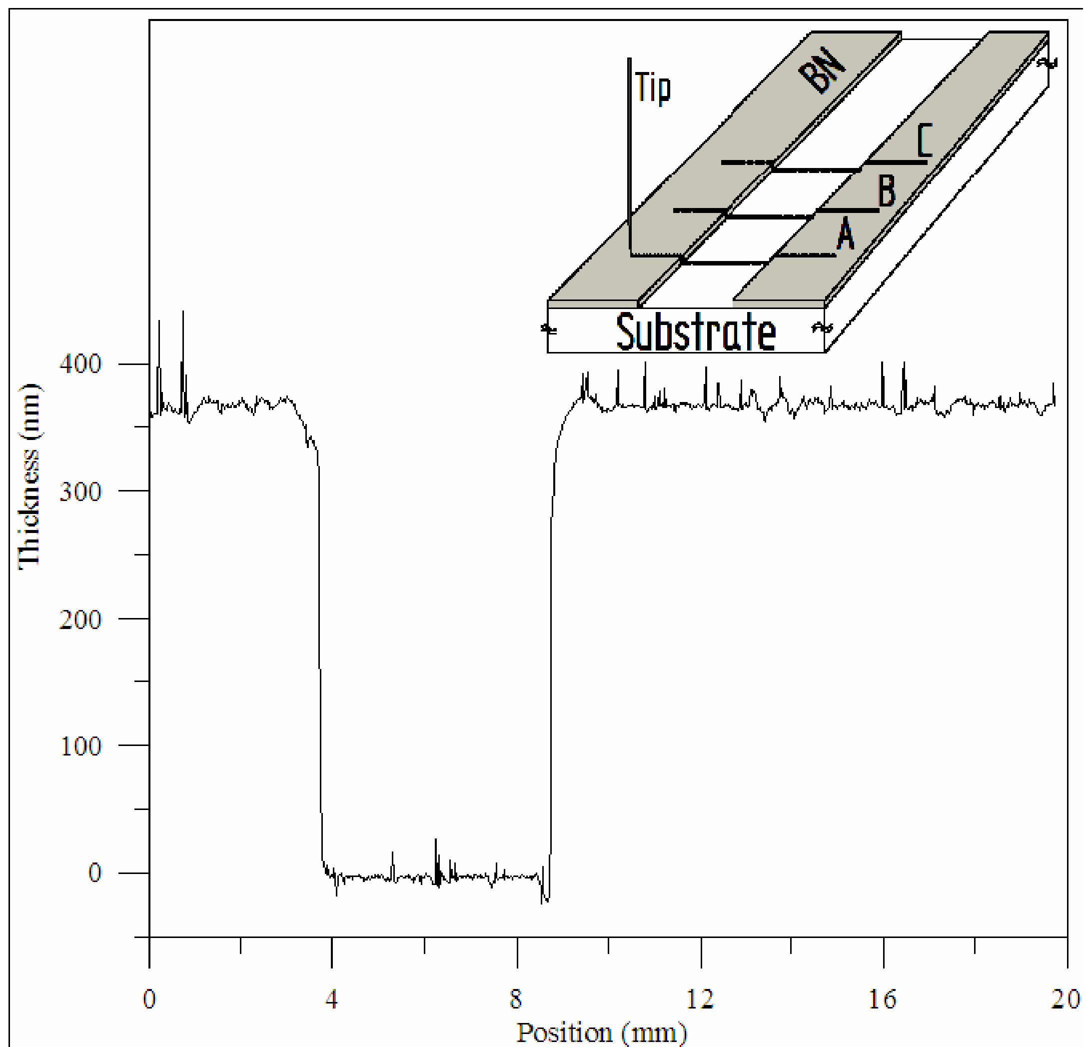

Figure 2.7. An example for the determination of the thickness and surface profile by the profilometer.

2.2.4. Mass Spectrometer

Hiden Analytical HPR 30 Quadrupol Mass Analyzer, shown in Figure 2.8 was used for the determination of the molecules in the residual gas and also it was used for the leakage control tests. The system is capable of detecting the masses between 0.4 and 300 atomic mass units (amu) with a resolution of 0.01 amu.

The HPR30 is a compact, bolt-on, in-situ process gas analyzer designed with the versatility to operate as a mobile or fixed station monitoring system in vacuum process applications. At the heart of the HPR30 system is the HPR30 Vacuum Manifold comprising an HPR30 inlet assembly and a mass spectrometer chamber [26].

The HPR30 inlet assembly consists of a stainless steel inlet block, two bellows sealed valves and a sampling tube incorporating a replaceable orifice.

A Conflat type DN-35-CF mounting flange is provided for mounting the HPR30 Manifold directly onto the slave unit of the PECVD system for accurate gas sampling. The HPR30 Manifold is configured for sampling process pressures up to 1 Torr via Process valve. Pressure reduction is achieved by a sampling orifice mounted in the end of the sampling tube. The HPR30 Manifold can also be used for sampling residual gases in the 5×10^{-5} Torr to Ultra High Vacuum (UHV) region by the Residual Gas Analysis (RGA) valve. Process monitoring or RGA operation is achieved by opening the appropriate valve as seen in Figure 2.9.

The HPR30 inlet assembly is fitted to a UHV mass spectrometer vacuum chamber into which is fitted the quadrupole mass spectrometer probe. The mass spectrometer vacuum chamber is evacuated by a 60 liter per second turbomolecular / drag (turbo) pump to provide a suitable vacuum in which the mass spectrometer can operate. The turbo pump is controlled by either a Turbo Interface and Power Unit or Turbo Interface Unit mounted in the electronics rack.

The HPR30 is mounted on a compact work station together with the electronic control units and backing pump.

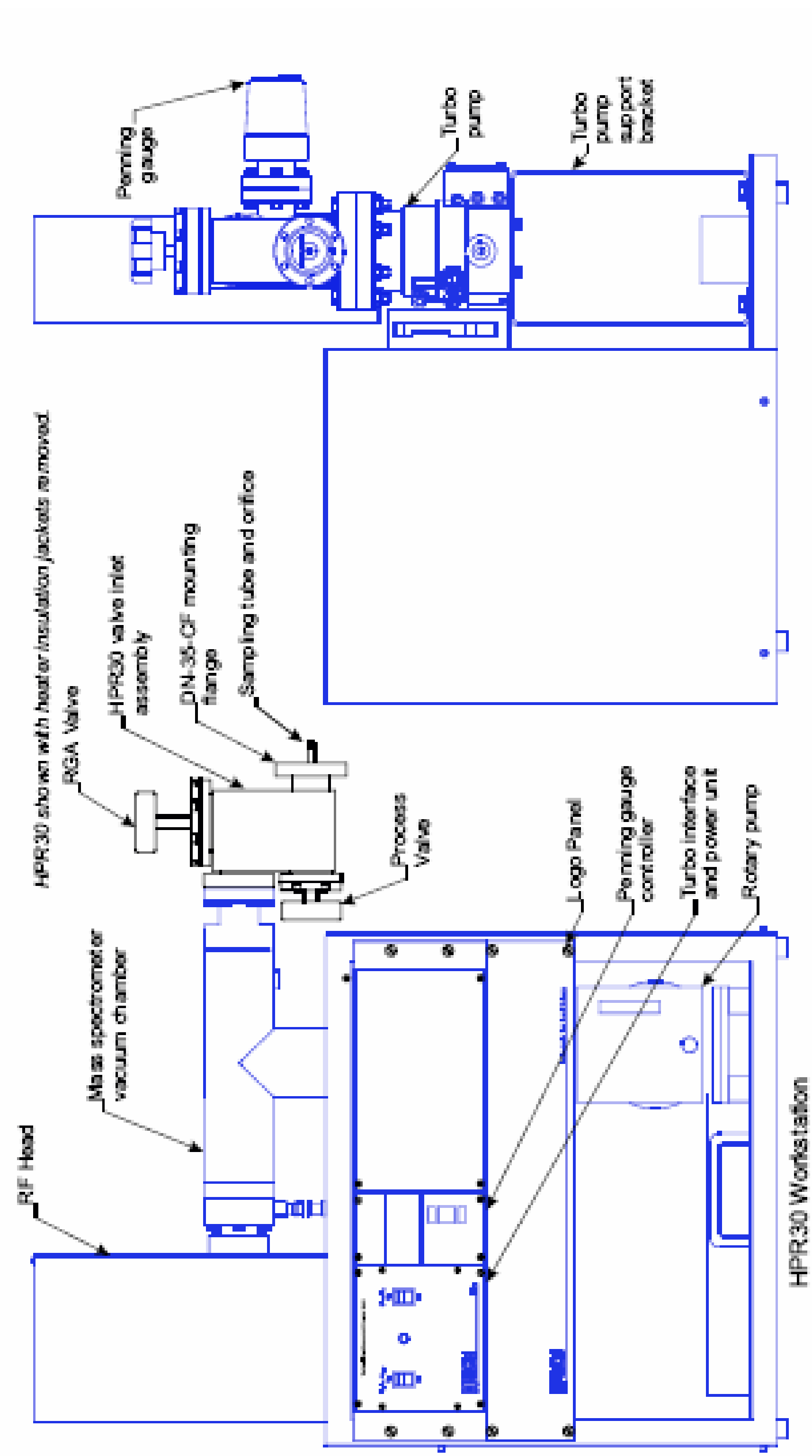

Figure 2.8. Typical HPR30 work station arrangement [26]

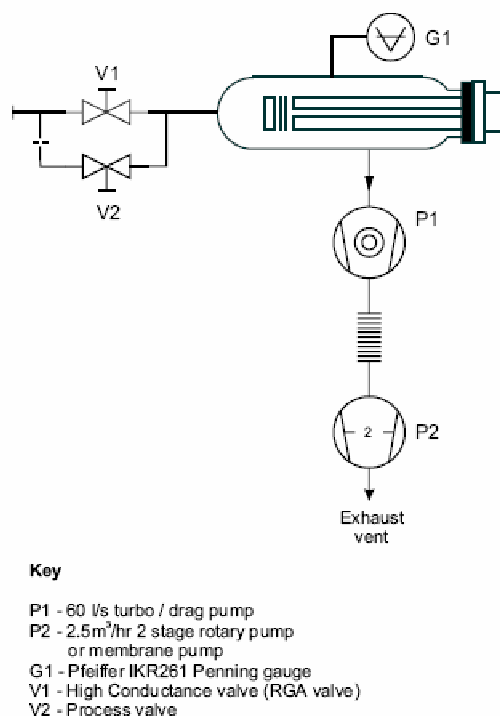

Figure 2.9. HPR30 vacuum schematic [26]

2.2.5. X-ray Photoelectron Spectrometer (XPS)

The chemical compositions of the films at the film surface were determined by the XPS analyzer Specs EA 200 at the Central Laboratory. The films deposited on 1x1 cm glass substrates were used for this purpose. The spectrometer has X-ray sources of both Al Kα (1486.3 eV) and Mg Kα (1253.6 eV). For the elimination of the carbon contamination on the surface, the films are sputtered with argon ions of energy 5000 eV for 15-20 minutes.

The photoemission process leads to positively charged ion formation at the surface. Those ions attract the ejected electrons back to the surface and thus reduce their kinetic energies. This attraction leads to the shift of the binding energies to higher energies in the XPS spectrum. The calibration of the peaks is done by using the

binding energy of a known compound [27]. Since C is almost always adsorbed on the surface, C 1s peak can be used for this purpose, which is located at 284.6 eV. However, since carbon is vanished in most of the experiments, the calibration is done according to B 1s peak, which is located at 190.5 eV [28]. Atomic sensitivity factors (ASF) of boron, oxygen, and nitrogen are taken as σ_B = 0.13, σ_O = 0.66, and σ_N = 0.42, respectively.

2.3. EXPERIMENTAL PROCEDURE

2.3.1. Substrate Cleaning

To determine structural and optical properties of the produced BN films, crystalline silicon (100) wafers polished on both sides, glass microscope slides and quartz plates are used as substrates. The deposition is susceptible to the cleanliness of the substrates, so a meticulous cleaning procedure must be performed. Glass and quartz cleaning procedure and silicon cleaning procedure are given below.

2.3.1.1. Glass and Quartz Cleaning Procedure

The main steps followed while glass and quartz cleaning were;

1. Boiling in detergent for 5 minutes.
2. Boiling in trichloroethylene (C_2HCl_3) for 3 minutes.
3. Boiling in H_2O_2:H_2O (1:1) solution for 3 minutes.

After each step, substrates were rinsed in deionized water (DW) and then washed in ultrasonic bath for 3 minutes.

2.3.1.2. Silicon Cleaning Procedure

The main steps followed while silicon cleaning were;

1. Boiling in H_2O : NH_4OH : H_2O_2 (6:1:1) mixture for 5 minutes.
2. Boiling in H_2O : HCl : H_2O_2 (6:1:1) mixture for 10 minutes.
3. Dipping in H_2O : HF (30:1) mixture for 30 seconds.
4. Drying with nitrogen gun.

After first and second steps, substrates were rinsed in DW and then washed in ultrasonic bath for 3 minutes. After third step, substrates were rinsed in running DW for 3 minutes.

After the cleaning process was over, the substrates were placed in the reactor immediately. Before the deposition process, the substrates were cleaned (etched) under nitrogen plasma for 5 minutes.

2.3.2. The PECVD Experiments

After cleaning, the substrates were immediately placed into the chamber and the system was taken into vacuum. At the same time, substrate temperature was adjusted for the master unit. When the pressure was reached 3-5 x 10^{-3} torr, N_2 flow of 100 ccm (cm^3/min) was introduced into the chamber. After process pressure was maintained at the chamber, substrates were etched in nitrogen plasma for 5 minutes. Consequently, the flow rates of the process gases, the deposition pressure, and bias voltage were set to the desired values. Plasma was formed by RF and/or MW power at desired power and the reaction was initiated. The experimental parameters were deposition pressure, substrate temperature, applied power, negative bias voltage applied to the substrates and the N_2/B_2H_6 gas ratio.

2.3.3. The Sputtering Experiments

After the substrate cleaning, the substrates were immediately placed into the chamber and the chamber was taken into high vacuum (10^{-9} bar). Then argon gas was introduced into chamber. When the pressure was reached 1-10 x 10^{-6} bar, plasma was formed by RF power at desired power and the deposition was initiated. The experimental parameters were deposition pressure and the RF power applied to the target.

CHAPTER 3

RESULTS AND DISCUSSIONS

3.1. THE ANALYSES OF THE FILMS DEPOSITED IN PECVD SYSTEM

3.1.1. The Analyses of The Films Deposited in The Master Unit of PECVD

While depositing thin films in the master unit of the PECVD system, pure nitrogen and diborane (B_2H_6) were used as the nitrogen and boron precursors. Double side polished silicon, glass and quartz were used as substrates. The deposition parameters of these experiments are given in Table 3.1.

3.1.1.1. FTIR Results

A typical IR spectra is given in Figure 3.1 with the deconvolution of the peaks attributed to the structures given in Table 3.2. Since there is significant height difference between peaks, B-H and N-H stretching vibration mode peaks are magnified in Figure 3.1. The spectrum mainly composed of absorption bands at around 900 cm^{-1}, 1300 cm^{-1}, 2500 cm^{-1} and 3500 cm^{-1} for the vibrations of B-N and B-H bending modes, B-N stretching mode including H and O bonds, B-H stretching mode and N-H stretching mode, respectively [29-33]. The peak named P4 and located at 1270 cm^{-1} could not be determined yet. However, in the literature it is both said that it is the boron-rich amorphous BN [34], and E-BN, where E stands for explosion [35,36]. The Structure of the E-BN was modelled to have both σ sp^3 and σ sp^2 chemical bonds (1:1) [35]. E-BN shows 2 peaks which are located at 927 and

1252 cm^{-1} [36] but no peak was observed at 927 cm^{-1} in the experiments, so the unknown peak is more likely to be boron-rich amorphous BN.

FTIR results are classified as six main deposition parameters such as the deposition pressure, substrate temperature, applied RF power, applied bias voltage to the substrates, N_2/B_2H_6 gas ratio and addition of argon gas to the process gases.

Table 3.1. Deposition parameters for the master unit of the PECVD

Experiment	RF (W)	Bias Voltage (V)	Flow Rates (cm^3/min)				Pressure (mTorr)	N_2/B_2H_6 Ratio (molar)	Substrate Temperature (°C)
			N_2	B_2H_6	Ar	Total			
B7	200	-80	18	30	-	48	500	4	250
B8	200	-250	18	30	-	48	500	4	250
B9	200	-100-200	18	30	-	48	100	4	250
B10	200	-100-150	30	20	-	50	100	10	250
B11	200	-130	40	10	-	50	100	25	250
B12	200	-	30	20	-	50	100	10	250
B13	270	-135-175	30	20	-	50	100	10	250
B14	200	-140-240	30	20	50	100	150	10	250
B15	200	-80-120	15	10	75	100	160	10	250
B38M	550	-	75	10	75	160	230	50	Room Temperature (R.T.)
B40	15	-	75	10	-	85	230	50	R.T.
B41	15	-	75	10	-	85	230	50	350
B42	15	-	75	10	-	85	230	50	250
B43	15	-	75	10	-	85	230	50	125

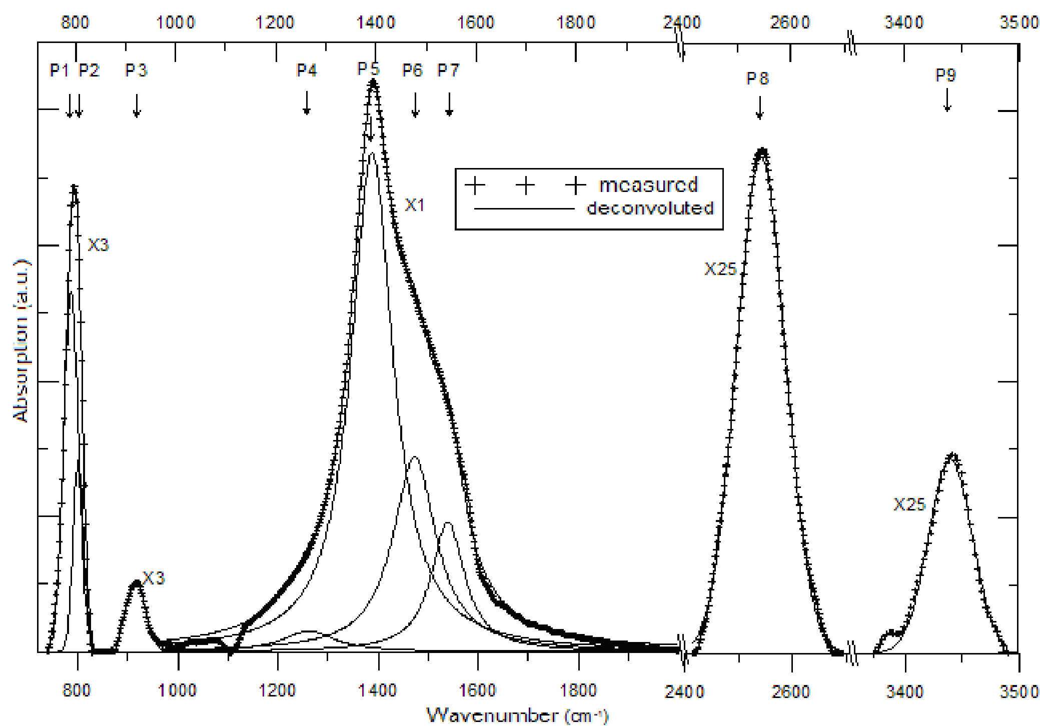

Figure 3.1 A typical IR spectra observed in experiments and the deconvolution of the peaks (B9 experiment)

Table 3.2. The wavenumbers of the peaks and corresponding vibrations [29-33]

Peak	**Wavenumber (cm^{-1})**	**Structure**
P1	783	B-N-B TO bending vibration mode (out of plane), sp^2 bonding
P2	828	B-N-B LO bending vibration mode(out of plane), sp^2 bonding
P3	905-920	B-H bending vibrational mode (out of plane)
P4	1270	Either of E-BN or Boron rich amorphous BN
P5	1380	B-N stretching vibration mode (in plane), sp^2 bonding transverse-optic (TO)
P6	1400-1500	B-O
P7	1500-1600	B-N stretching vibration mode (in plane), sp^2 bonding longitudunal-optic (LO)
P8	2535	B-H stretching vibration mode
P9	3435	N-H stretching vibration mode

While passing through B8 to B9, the pressure was reduced from 0.5 Torr to 0.1 Torr. The deposition parameters of these experiments are given in Table 3.3, and their IR spectrum are shown in Figure 3.2.

As seen in Figure 3.2, decreasing the deposition pressure leads to less N-H and B-H bond formation in the film. With decreasing the pressure, the ion energies in the plasma increases and these ions etches weak bonds such as N-H and B-H. So, the hydrogen contamination in the film got lower with decreasing the pressure.

Table 3.3. Deposition parameters of B8 and B9 experiments

Parameters	B8	B9
Substrate Temperature (°C)	250	250
Pressure (Torr)	0.5	0.1
Power (W)	200	200
Bias Voltage (V)	~ -250	~ -200
N_2/B_2H_6 (molar)	4	4

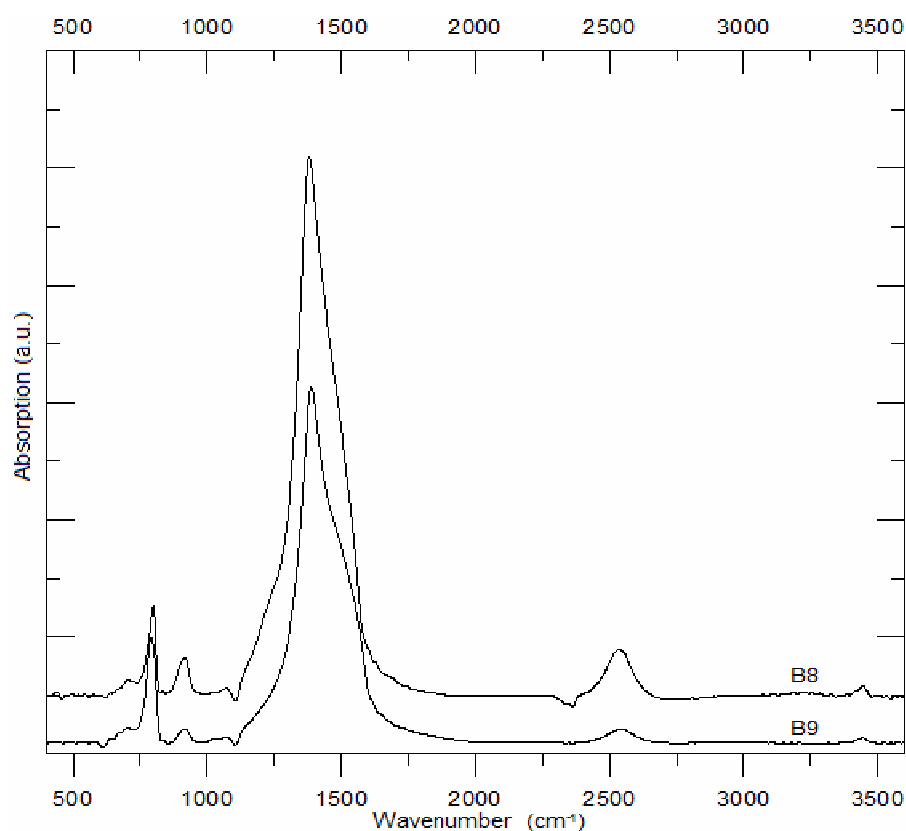

Figure 3.2 The effect of pressure on IR spectrum of B8 and B9 experiments

In B40, B43, B42 and B41 experiments, the effects of temperature were investigated. The deposition parameters of these experiments are given in Table 3.4, and their IR spectrum are shown in figures 3.3, 3.4, 3.5 and 3.6, respectively.

Tablo 3.4. The deposition parameters of B40, 41, 42 and 43 experiments

Parameters	B40	B41	B42	B43
Substrate Temperature (°C)	23	350	250	125
Pressure (Torr)	0.23	0.23	0.23	0.23
Power (W)	15	15	15	15
Bias Voltage (V)	-	-	-	-
N_2/B_2H_6 (molar)	50	50	50	50

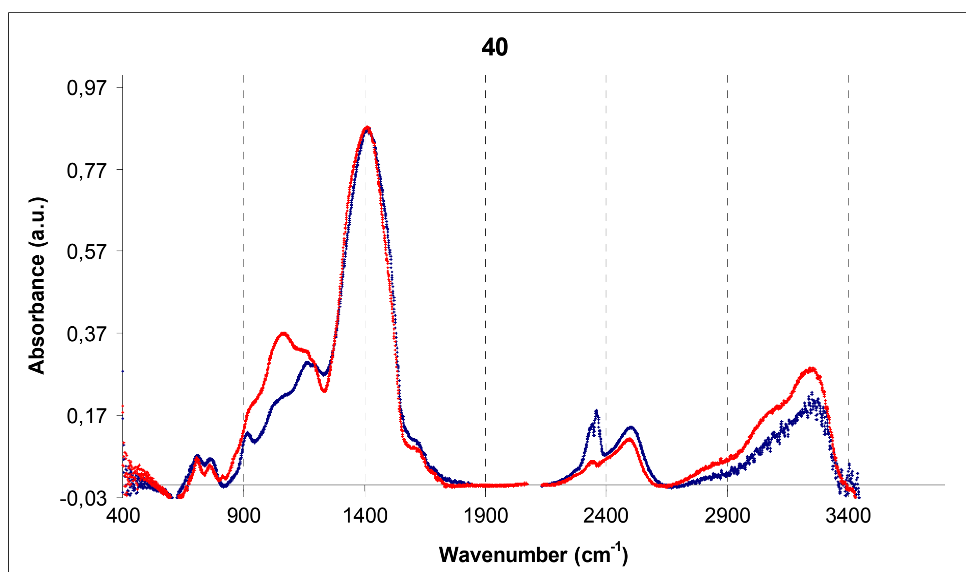

Figure 3.3. The spectrum of B36 experiment, which was carried out at room temperature, at the deposition day (blue) and 3 days after the deposition (red)

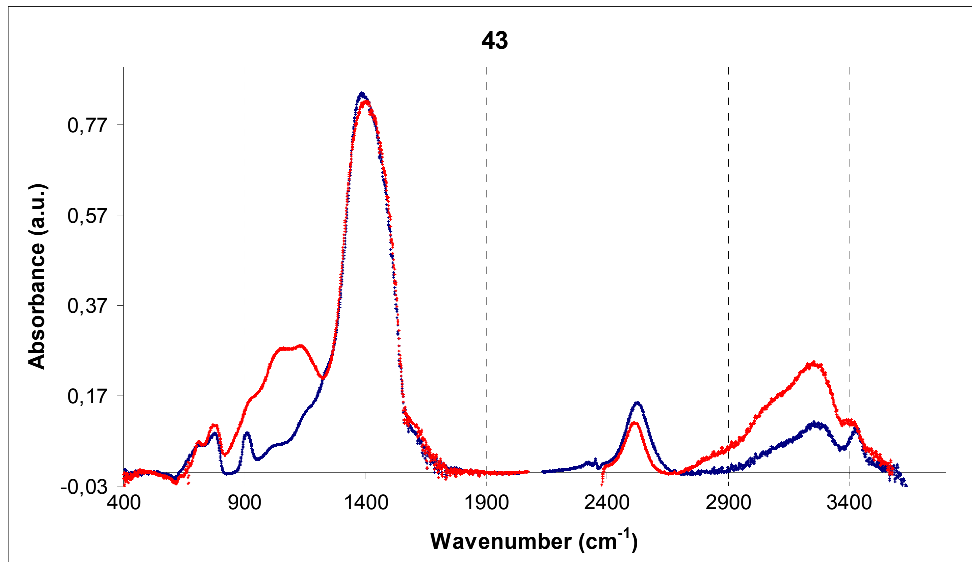

Figure 3.4. The spectrum of B36 experiment, which was carried out at 125 °C, at the deposition day (blue) and 3 days after the deposition (red)

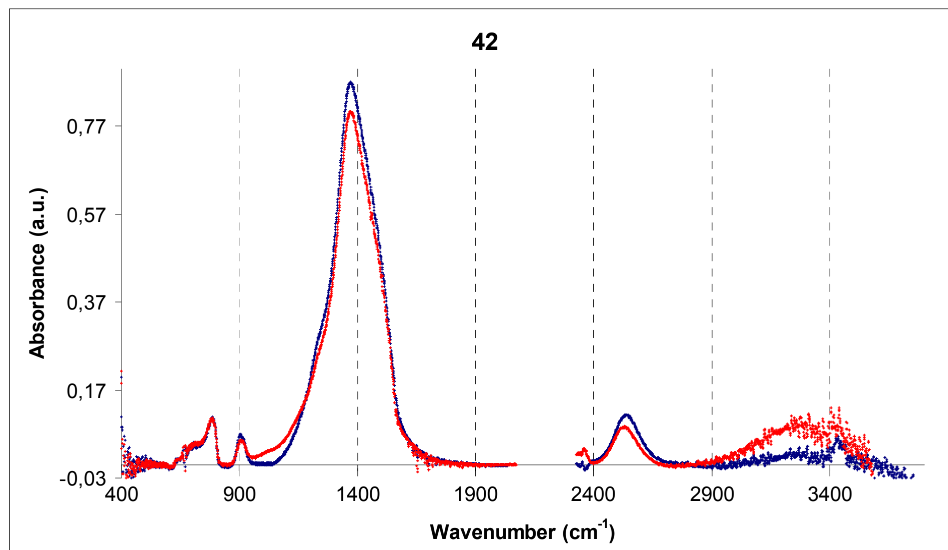

Figure 3.5. The spectrum of B36 experiment, which was carried out at 250 °C, at the deposition day (blue) and 3 days after the deposition (red)

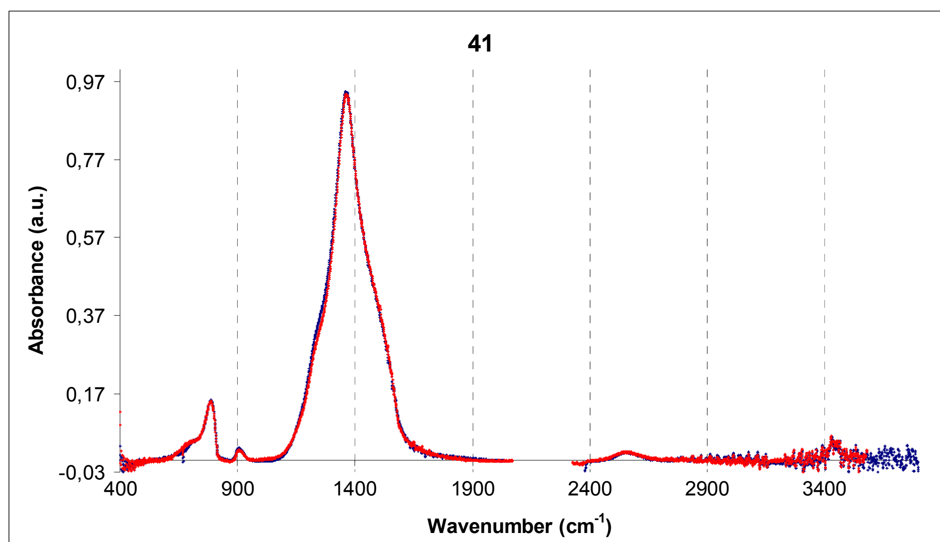

Figure 3.6. The spectrum of B36 experiment, which was carried out at 350 °C, at the deposition day (blue) and 3 days after the deposition (red)

From Figure 3.3 through Figure 3.6, the change of IR spectrum of films deposited at different substrate temperatures in 3 days are seen. Increase in the substrate temperature led to less change in the spectrum, so led to the more stable films.

While passing through B10 to B13, the applied RF power was increased from 200 W to 270 W. The deposition parameters of these experiments are given in Table 3.5, and their IR spectrum are shown in Figure 3.7.

Table 3.5. The deposition parameters of B10 and B13 experiments

Parameters	**B10**	**B13**
Substrate Temperature (°C)	250	250
Pressure (Torr)	0.1	0.1
Power (W)	200	270
Bias Voltage (V)	~ -150	~ -150
N_2/B_2H_6 (molar)	10	10

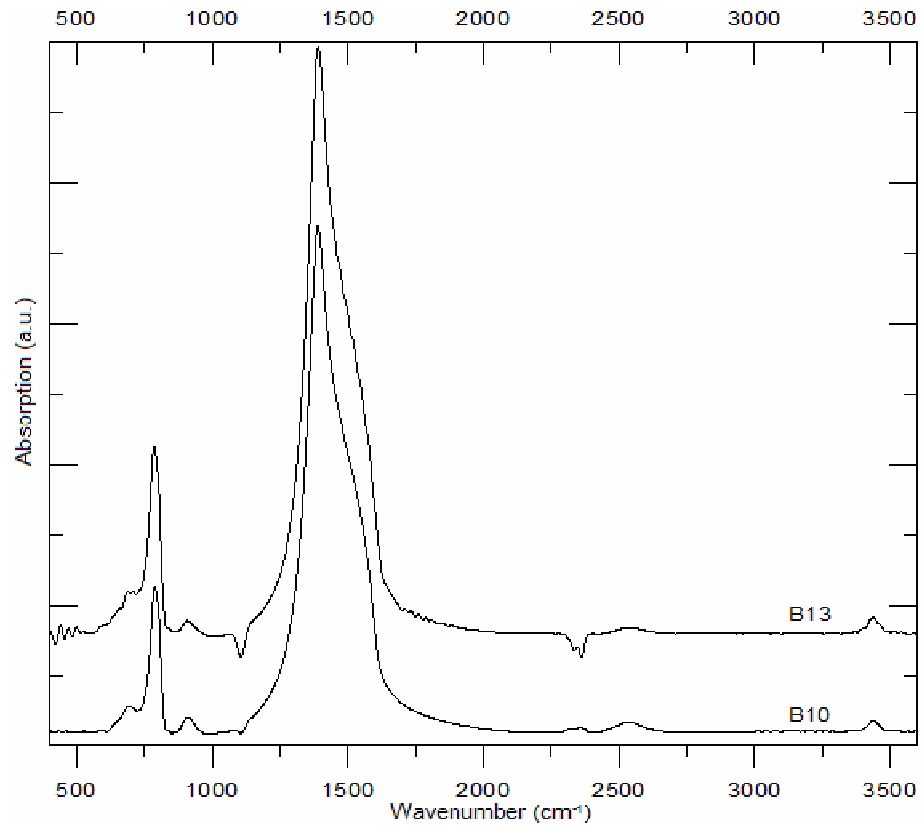

Figure 3.7. The effect of applied power on IR spectrum of B10 and B13 experiments

It is clearly seen in Figure 3.7 that the increase of RF power does not have a significant effect on hexagonal film deposition since the h-BN peaks did not show any difference.

In B10 experiment, -150 V bias voltage was applied to the substrates, whereas in B12 experiment no voltage was applied to the substrates. The deposition parameters of these experiments are given in Table 3.6, and their IR spectrum are shown in Figure 3.8.

Table 3.6. The deposition parameters of B10 and B12 experiments

Parameters	B10	B12
Substrate Temperature (°C)	250	250
Pressure (Torr)	0.1	0.1
Power (W)	200	200
Bias Voltage (V)	~ -150	-
N_2/B_2H_6 (molar)	10	10

The applied negative voltage accelerated the positive ions in the plasma to the substrates. So, negative bias voltage led to the more BN bond formation as seen in absorptions peaks in Figure 3.8.

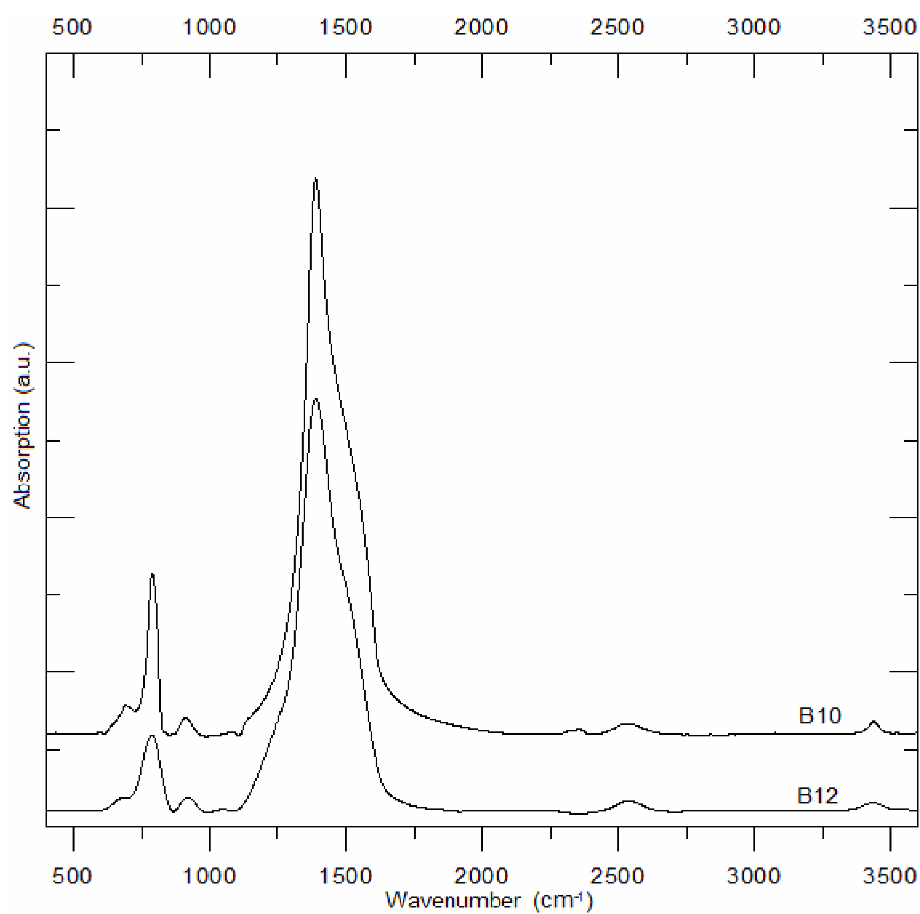

Figure 3.8. The effect of applied bias voltage on the substrates on IR spectrum of B10 and B12 experiments

N_2/B_2H_6 gas ratio was increased from B9 experiment through B11 experiment. The deposition parameters of these experiments are given in Table 3.7, and their IR spectrum are shown in Figure 3.9.

Table 3.7. The deposition parameters of B9, B10 and B12 experiments

Parameters	B9	B10	B11
Substrate Temperature (°C)	250	250	250
Pressure (Torr)	0.1	0.1	0.1
Power (W)	200	200	200
Bias Voltage (V)	~ -150	~ -150	~ -150
N_2/B_2H_6 (molar)	4	10	25

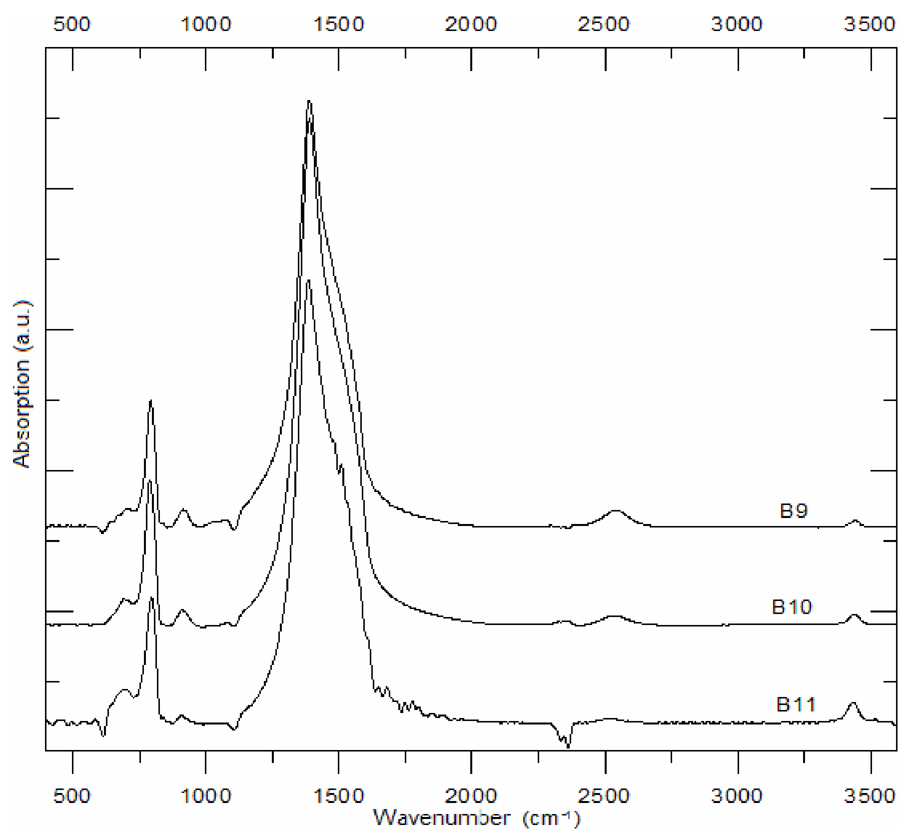

Figure 3.9. The effect of N_2/B_2H_6 ratio on IR spectrum of B9, B10 and B11 experiments

As clearly seen from Figure 3.9, with increasing N_2/B_2H_6 ratio, the N-H bond formation also increases, whereas the B-H bond formation decreases.

Argon gas was added in an increasing manner to the process gases in B14 and B15 experiments. The deposition parameters of these experiments are given in Table 3.8, and their IR spectrum are shown in Figure 3.10.

Addition of argon gas to the process gases or the increase of the argon amount in the process gases did not lead to a significant effect on the hexagonal structure formation as seen in Figure 3.10.

Table 3.8. The deposition parameters of B10, B14 and B15 experiments

Parameters	**B10**	**B14**	**B15**
Substrate Temperature (°C)	250	250	250
Pressure (Torr)	0.1	0.15	0.15
Power (W)	200	200	200
Bias Voltage (V)	~ -150	~ -150	~ -100
N_2/B_2H_6 (molar)	10	10	10
N_2/Ar (molar)	-	0.6	0.2

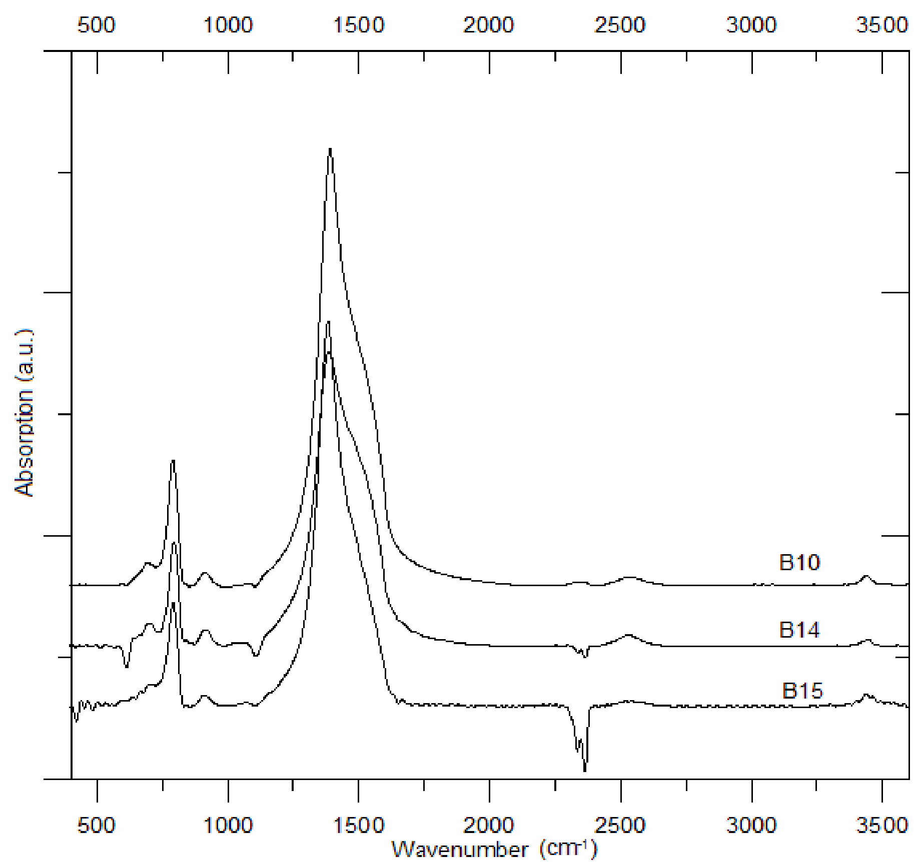

Figure 3.10. The effect of argon addition to the process gases on IR spectrum of B10, B14 and B15 experiments

3.1.1.2. UV-Vis Results

The energy amount that is necessary for a semi-conductor to start electrical conduction is called forbidden energy band-gap, which is also known as the energy distance between conduction and valence bands in a semi-conductor. For the determination of the forbidden energy band-gaps, absorption coefficients of the films were calculated by using the formula;

$$\alpha = -\ln(T/T_0)/d \qquad \text{(Eqn. 3.1)}$$

Where α is the absorption coefficient, T is the transmission and d is the thickness of the film.

At the α of 10^4 cm^{-1}, there are no more interference fringes. So the energy corresponding to the α of 10^4 is taken as a measure of the forbidden band-gap and results are tabulated in Table 3.9.

Table 3.9. The forbidden band-gaps of the experiments

Experiment	Forbidden Band-Gap (eV)
B7	2.12
B8	4.64
B9	4.16
B10	4.71
B11	4.81
B12	4.64
B13	4.56
B14	3.63
B15	4.90
B40	4.96
B41	4.98
B42	4.64
B43	5.06

3.1.1.3. Profilometer Results

The measured film thicknesses by profilometry and the average deposition rates are given in Table 3.10.

Table 3.10. The thicknesses and the deposition rates of the B7-15 experiments

Experiment	Thickness (nm)	Deposition Rate (nm/min)
B7	700-750	14-15
B8	600-1000	12-20
B9	500-600	8.9-10.7
B10	500-600	9.1-10.9
B11	350-550	3.9-6.1
B12	580-650	9.7-10.8
B13	370-650	8.2-14.4
B14	500-1000	7.7-15.4
B15	200-350	4.8-8.3
B40	710	11.8
B41	310	5.2
B42	450	7.5
B43	690	11.5

From B7 to B15, the thicknesses were measured from the center to the edge of the electrode. The nonuniformity in the reactor could be seen from Table 3.10. The maximum values were obtained from the center and the minimum values were observed at the edges. The last four thicknesses were measured from the center of the electrode.

3.1.1.4. XPS Results

The films were sputtered with argon ions of 5000 eV for about 20 minutes for the elimination of the carbon atoms on the surface by etching a little layer on the film before the XPS measurements. A typical XPS spectra after the elimination of the carbon contamination is given in Figure 3.11. These 3 peaks are boron (B 1s), nitrogen (N 1s) and oxygen (O 1s) from lower to higher energies, respectively. Before the calculations, first of all a baseline correction was made to the spectra and then the energy levels were shifted according to the B 1s (190.5 eV) peak [28]. The atom concentrations on the surfaces were calculated by the peak areas and the atomic sensitivity factors. The results are given in Table 3.11. The XPS measurements could be made in two months after the depositions. During this time the BN films caught water vapor from the atmosphere and formed ammonium borate hydrate structures as observed earlier in the literature [37]. The high oxygen amount on the surfaces is considered to be occur for this reason.

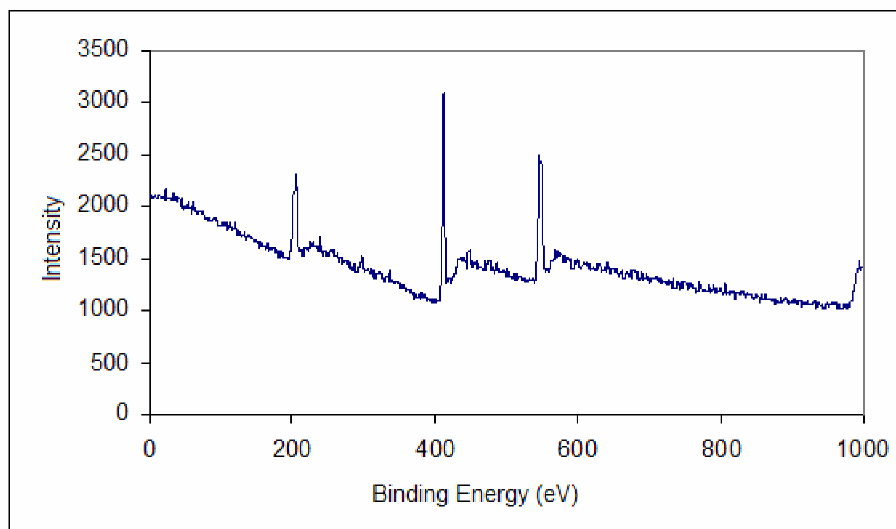

Figure 3.11. A typical XPS spectra (B10 experiment)

Table 3.11. The surface concentrations and atom ratios of B7-B15 experiments

Experiment	Surface Concentration (%)				Atom Ratio	
	B	N	O	C	N/B	O/B
B7	48.4	15.4	28.8	7.4	0.318	0.595
B8	37.4	28.1	34.5	-	0.752	0.922
B9	55.2	35.4	9.4	-	0.641	0.170
B10	55.4	35.6	9.0	-	0.641	0.160
B11	51.7	36.4	11.9	-	0.704	0.230
B12	50.3	38.4	11.3	-	0.765	0.225
B13	49.9	33.8	12.3	4.0	0.678	0.247
B14	58.2	14.1	25.3	2.4	0.242	0.435
B15	53.9	16.3	26.7	3.1	0.303	0.496
B40	54.95	10.06	34.99	-	0.18	0.64
B41	62.86	21.99	15.15	-	0.35	0.24

The film deposited at 350 ºC (B41) has less oxygen contamination when compared to the film deposited at room temperature (B40). At higher temperatures the crystals were observed to be better oriented, so the chance to catch any contaminant is less probable.

3.1.1.5. The Investigation of the Films Deposited By the Master Unit of PECVD

In the master unit of the PECVD system, hexagonal boron nitride thin films were deposited. The effects of the determined parameters on the film structure, deposition rate, surface concentrations, and forbidden band-gaps are discussed below.

3.1.1.5.1. The Effect of Pressure on the Deposited Films in the Master Unit of the PECVD System

Decreasing the deposition pressure from 500 mTorr to 100 mTorr (B8 and B9 experiments) was led to a decrease in the B-H and N-H bonds in the film structure as

seen in Figure 3.2. However, with reducing the deposition pressure, film deposition rate was significantly decreased as seen in Table 3.10.

3.1.1.5.2. The Effect of the Applied RF Power on the Deposited Films in the Master Unit of the PECVD System

Increasing the RF power applied to the upper electrode from 200 W to 270 W did not have any effect on the hexagonal structure as seen from Figure 3.7. The maximum RF power, which is 300W, that the system can handle was nearly reached, but no structural change was observed. On the other hand, power increase led to higher film deposition rates because more energy was present in the chamber for species to react rapidly, as seen in Table 3.10.

3.1.1.5.3. The Effect of N_2/B_2H_6 Gas Ratio on the Deposited Films in the Master Unit of the PECVD System

Increasing the N_2/B_2H_6 ratio led to an increase in the N-H bonds in the film structure. On the other hand, the B-H bonds were decreasing as seen from Figure 3.9. When this ratio has reached 25, the film deposition rate was significantly decreased as seen from Table 3.10. XPS results showed that the nitrogen concentration on the surface was slightly increasing with increasing the ratio as seen from Table 3.11. However, the ratio change could not affect the forbidden energy band-gaps of the films.

3.1.1.5.4. The Effect of Temperature on the Deposited Films in the Master Unit of the PECVD System

Increasing the substrate temperature led to more stable film structures. As seen in the figures 3.3, 3.4, 3.5 and 3.6, with increasing the substrate temperature, both N-H and B-H bonds were decreased. Moreover, the change of the structure, therefore the delamination of the films got slowed down. Since the films were found out to be chemically more stable, there was less chance to capture water vapor from the air. So, the N/B atom ratio on the film surfaces was observed to be increased with

temperature as seen from Table 3.11. However, the film deposition rate was found to be decreased with increasing substrate temperature as seen from Table 3.10.

3.1.1.5.5. The Effect of the Applied Bias Voltage on the Deposited Films in the Master Unit of the PECVD System

Applying negative bias voltage attracted positive ions to the substrates, so the BN bonds in the films were increased as seen in Figure 3.8. Applying bias voltage has increased the forbidden energy band-gap of the films as given in Table 3.9, however; it has no effect on the film depositon rates as given in Table 3.10.

3.1.1.5.6. The Effect of Addition of Argon Gas to the Process Gases on the Deposited Films in the Master Unit of the PECVD System

Addition of argon gas to the process gases did not have any effect on the hexagonal structure of the BN films as seen in Figure 3.11. Since argon gas acts as an etchant in the plasma medium, it etched the weak bonds in the films. So, the increase of argon amount in the gas mixture led to a decrease in the film deposition rate as seen in Table 3.10. Since weak bonds were eliminated, this increase also led to an increase in the forbidden energy band-gaps when argon amount exceeded the nitrogen amount in the gas mixture as seen in Table 3.9. Addition of argon gas to the process gas mixture decreased the nitrogen concentration on the surface significantly as seen from Table 3.11.

3.1.2. The Analyses of the Deposited Films in the Slave Unit of the PECVD

While depositing thin films in the slave unit of the PECVD system, pure nitrogen and diborane (B_2H_6) were used as the nitrogen and boron precursors. Double side polished silicon, glass and quartz were used as substrates. The deposition parameters of these experiments are given in Table 3.12.

Table 3.12. Deposition parameters for the slave unit of the PECVD

Experiment	RF (W)	Bias Voltage (V)	Flow Rates (cm^3/min)				Pressure (mTorr)	N_2/B_2H_6 Ratio (molar)
			N_2	B_2H_6	Ar	Total		
B16	-	-	30	20	-	50	93	10
B17	-	-	30	20	-	50	1000	10
B18	190	160	30	20	-	50	95	10
B19	230	-	30	20	-	50	95	10
B20	-	-	30	20	-	50	150	10
B21	210	100	30	20	-	50	93	10
B22	-	-	30	20	-	50	93	10
B23	-	-	30	20	-	50	97	10
B24	225	25	30	20	-	50	95	10
B25	100	160	30	20	-	50	97	10
B26	100	160	39.4	10.6	-	50	95	25
B27	100	205	15	10	25	50	95	10
B28	100	205	75	10	25	110	150	50
B29	100	200	160	10	25	195	180	100
B30	100	230	160	10	-	170	187	100
B31	40	100	75	10	75	160	185	50
B32	100	210	160	10	-	170	183	100
B33	30	100	75	10	75	160	183	50
B34	95	95	11	74	75	160	175	1
B35	90	150	-	110	-	110	160	-
B36	230	310	75	10	75	160	180	50
B37	120	-	75	10	75	160	175	50
B38İ	550	350	75	10	75	160	215	50
B39	-	200	30	20	-	50	185	10

3.1.2.1. FTIR Results

The B17, B23, B26 and B28 experiments were taken as typical experiments in MW PECVD system and their deposition parameters are given in Table 3.13, and their IR spectrum are given below in the figures 3.12 to 3.15.

Table 3.13. The deposition parameters of the B17, 23, 26 and 28 experiments

Experiment		B17	B23	B26	B28
MW		On	On	On	On
RF (W)		-	-	100	100
Bias Voltage (V)		-	-	160	205
Flow Rates (cm^3/min)	N_2	30	30	39.4	75
	B_2H_6	20	20	10.6	10
	Ar	-	-	-	25
	Total	50	50	50	110
Pressure (mTorr)		1000	100	100	150
N_2/B_2H_6 ratio (molar)		10	10	25	50

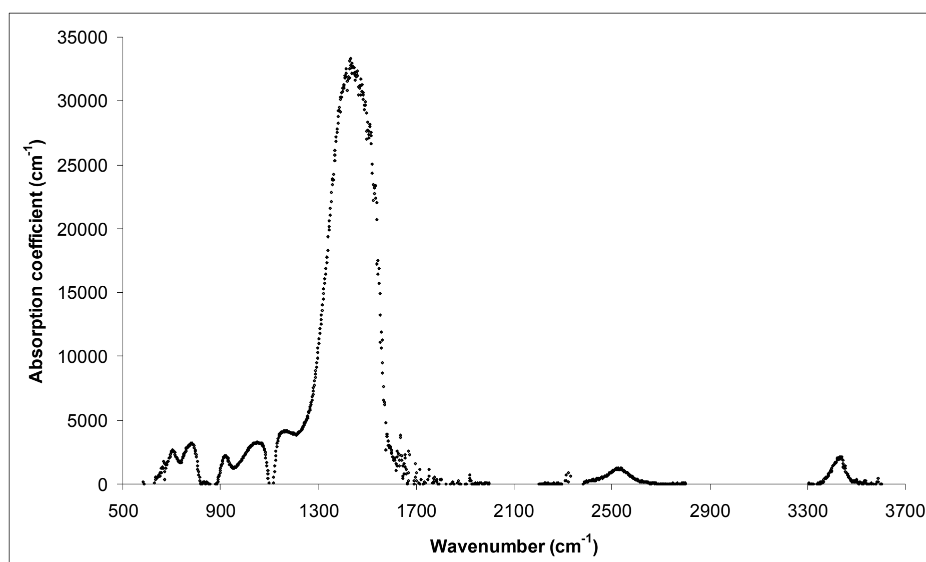

Figure 3.12. The IR spectra of the B17 experiment

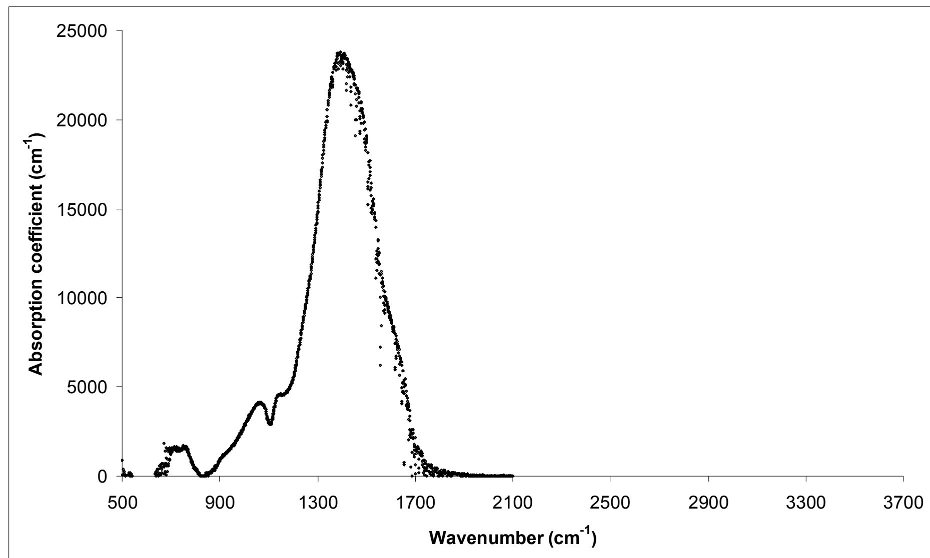

Figure 3.13. The IR spectra of the B23 experiment

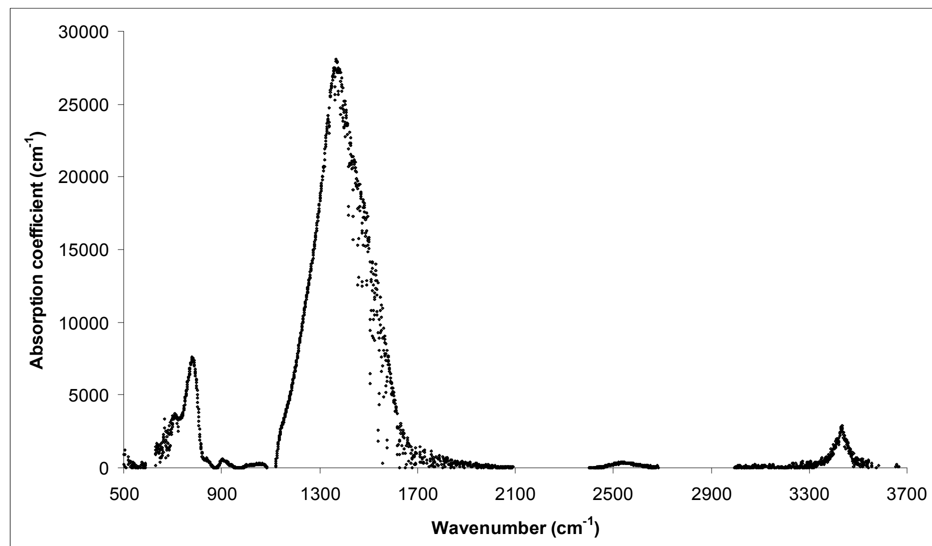

Figure 3.14. The IR spectra of the B26 experiment

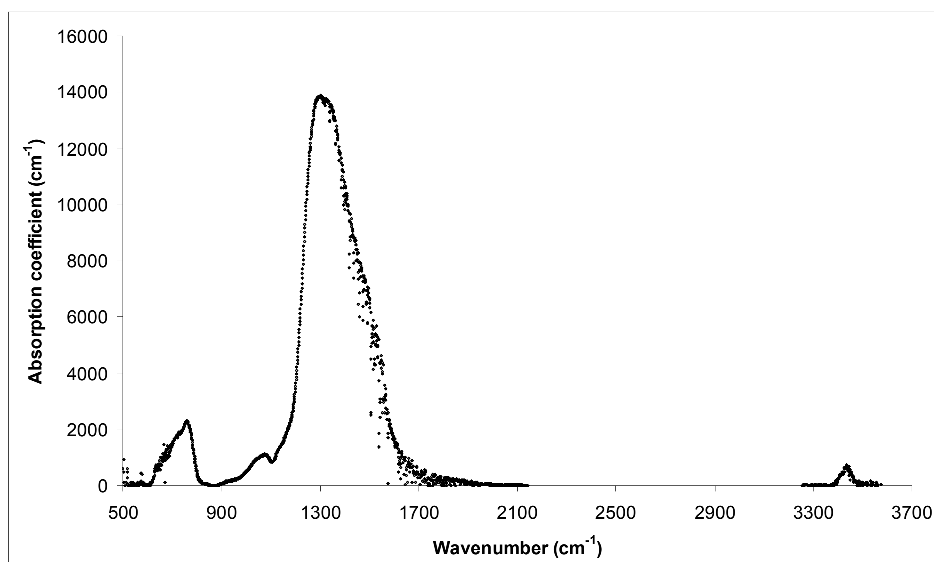

Figure 3.15. The IR spectra of the B28 experiment

When only MW was used as the power supply, a different IR spectra was observed. As an example of this characteristic, figures 3.12 and 3.13 are given for B17 and B23 experiments. In these figures narrow h-BN peaks were observed. However, a peak formation located at the wavenumber of 1100 cm^{-1} was seen, which is the characteristic vibration of c-BN. Moreover, in B23 experiment, the B-H peak vanished with decreasing the deposition pressure from 1 Torr to 0.1 Torr, but it has decreased the absorption coefficient, so the number of BN bonds.

The B26 and B28 experiments were carried out by using both of the power supplies (MW and RF). The resulting spectrum are shown in the figures 3.14 and 3.15. The IR spectra of B26 experiment is shown in Figure 3.14. In this figure, the characteristic peaks of h-BN located at 1375 cm^{-1} ve 800 cm^{-1} wavenumbers showed a narrower behaviour than the B17 and B23 samples. It implies that the addition of RF power to the MW led to better ordered h-BN structure in the films. On the other hand the cubic peak located at 1070 cm^{-1} was vanished.

Effect of argon dilution on bonding properties is depicted in Figure 3.15, where a wide absorption peak around 1300 cm^{-1} is shown for the B28 experiment. Addition of argon gas to the process gases has broadened the h-BN peaks and decreased the absorption coefficient.

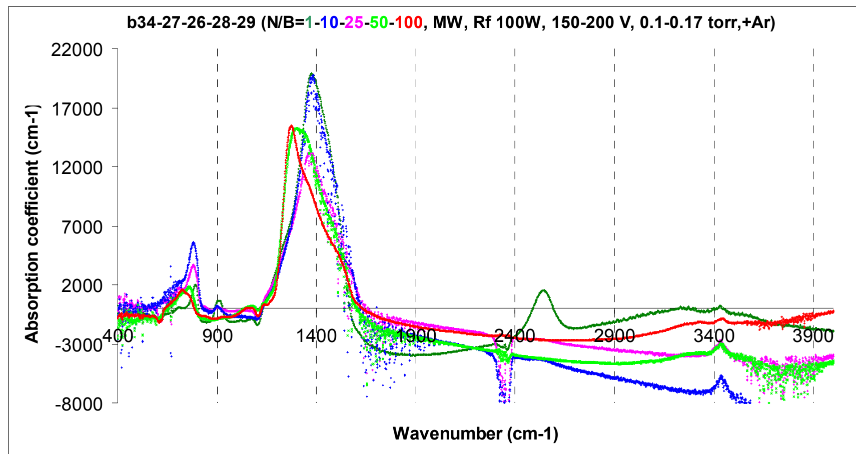

Figure 3.16. The spectrum of films deposited at different N_2/B_2H_6 gas ratios

The IR spectrum of the experiments B34, 27, 26, 28, 29 in which different N_2/B_2H_6 gas ratios were used are given in Figure 3.16. The increase in this ratio has increased the intensity of the peak located at 1270 cm^{-1}, which was undesired because the peak probably shows boron-rich amorphous BN structure [34].

The change of the IR spectrum of B22 experiment with respect to time is shown In Figure 3.17. This spectrum shows a typical structural change in a time span of 7 months and peeling off from the substrate for most of the deposited films.

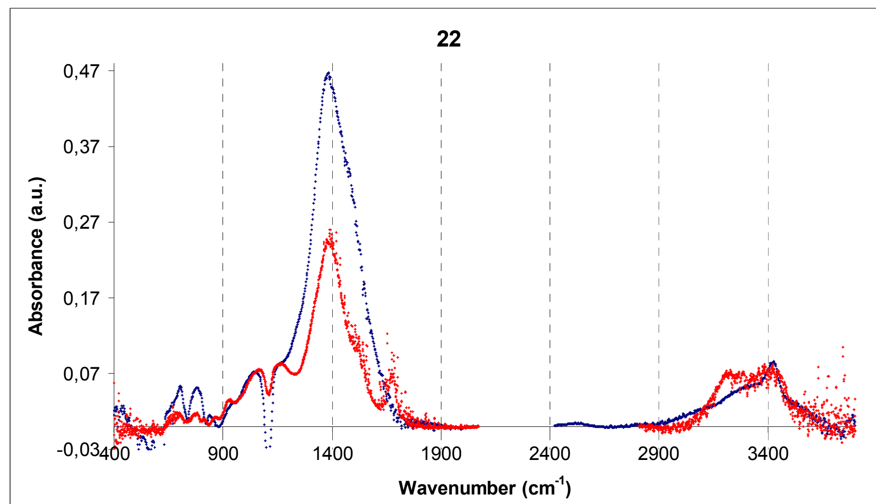

Figure 3.17. The spectrum of B22 experiment at the deposition day (blue) and 7 months after the deposition (red)

The broad peaks located at 800-1200 cm^{-1} and 1680 cm^{-1} and 2900-3500 cm^{-1} in B22 arose with time as seen in Figure 3.17. These peaks point out that ammonium borate hydrate structure formation occurs in the films when the films were exposed to atmosphere as it is stated in literature [37].

The stability of the B36 experiment seen in Figure 3.18 is considered to be based on the negative bias voltage applied to the substrates.

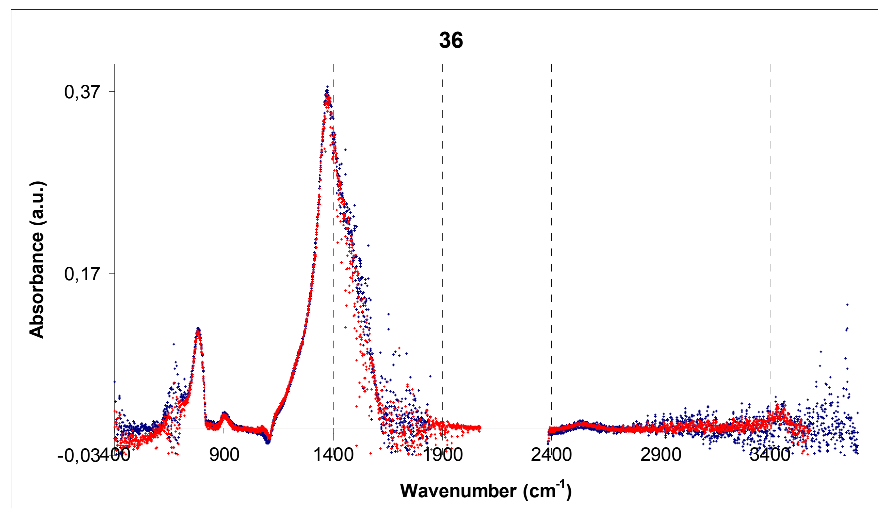

Figure 3.18. The spectrum of B36 experiment at the deposition day (blue) and 15 days after the deposition (red)

3.1.2.2. UV-Vis Results

For the determination of the forbidden energy band-gaps, absorption coefficients of the films were calculated by using Eqn 3.1.

The energy corresponding to the α of 10^4 cm^{-1} was taken as a measure of the forbidden band-gap and results are tabulated in Table 3.14.

Table 3.14. The forbidden band-gaps of the experiments

Experiment	Forbidden Band-Gap (eV)
B16	4.70
B18	3.68
B19	4.66
B22	4.49
B23	4.31
B24	3.67
B25	4.63
B26	4.29
B33	5.99
B34	2.99
B35	1.86
B36	4.38
B38	5.15

3.1.2.3. Profilometer Results

The measured film thicknesses by profilometry and the average deposition rates are given in Table 3.15.

Table 3.15. The thicknesses and the deposition rates of the experiments

Experiment	Thickness (nm)	Deposition Rate (nm/min)
B16	1250	16.7
B18	150	4.5
B19	3060	38.2
B22	190	6.3
B23	370	14.8
B24	260	8.1
B25	440	14.7
B26	190	3.6
B33	550	14.9
B34	350	11.7
B35	1000	40.0
B36	165	3.7
B38	240	5.3

3.1.2.4. Mass Spectrometer Results

The peaks seen in the mass spectrum below are labelled according to the elements in Table 3.16.

Table 3.16. The observed peaks in the mass spectrum and the corresponding molecules

Element	Peak (amu)
Nitrogen	14,28,29
Diborane	10,11,12,13,22,23,24,25,26,27
Oxygen	16,32
Hidrogen	1,2
Argon	20,40
Water Vapor	16,17,18

To determine if the mass spectrometer could be used as a gas leakage detector or not, a string of hair was placed on the gasket of the top cover of the plasma chamber. When a sample of acetone was injected through this artificial leak, the mass spectra shown in Figure 3.19 was observed. The peak located at 43 amu is the most intense peak for the acetone. As a result of this experiment, since the aceton peaks were seen in the mass spectra, mass spectrometer is found out to be a perfect instrument for leakage controls.

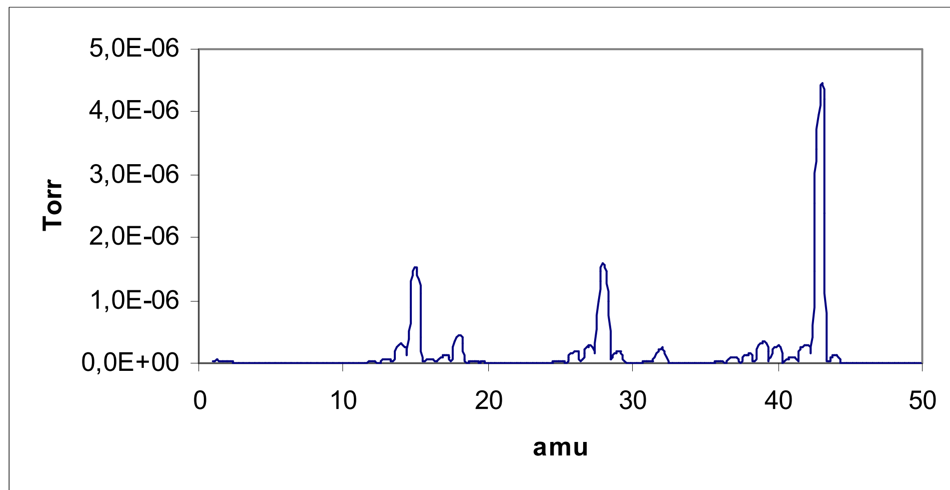

Figure 3.19. The mass spectra observed when a string of hair was placed on the gasket of the cover of the plasma chamber

So, the mass spectrometer was used to check air leakage into the system. The helium gas was injected to every point of the reactor for the determination of the leaking parts. According to the leaking part, either the gaskets were renewed or the leaking parts were welded. It is possible to follow these steps in figures 3.20 to 3.23. In B19, the nitrogen and the oxygen peaks (28 and 32 amu) are relatively high when compared to the background water vapor as seen in Figure 3.20. These peaks got lower with avoiding the leaks. It is understood from Figure 3.23 that there was no air leakage in the B39 experiment, only the background of water vapor located at 16, 17 and 18 amu.

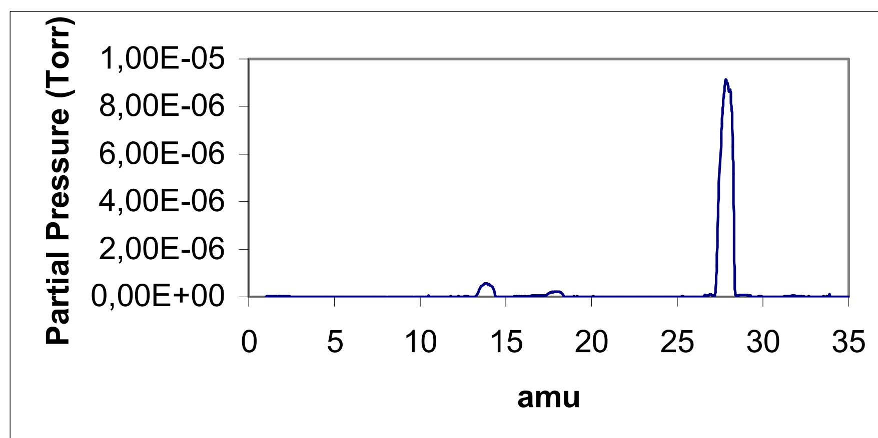

Figure 3.20. The mass spectra of B19 experiment before the process gases were given to the chamber (high partial pressure of nitrogen, peak located at 28 amu)

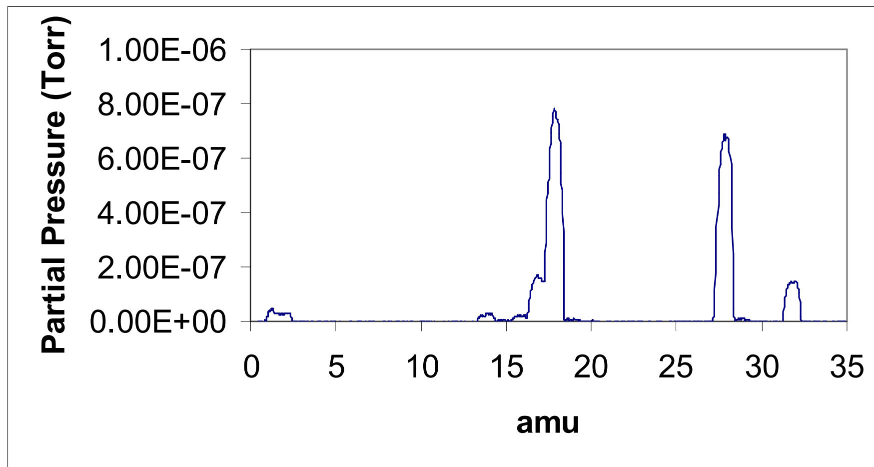

Figure 3.21. The mass spectra of B26 experiment before the process gases were given to the chamber (moderate partial pressure of nitrogen, peak located at 28 amu)

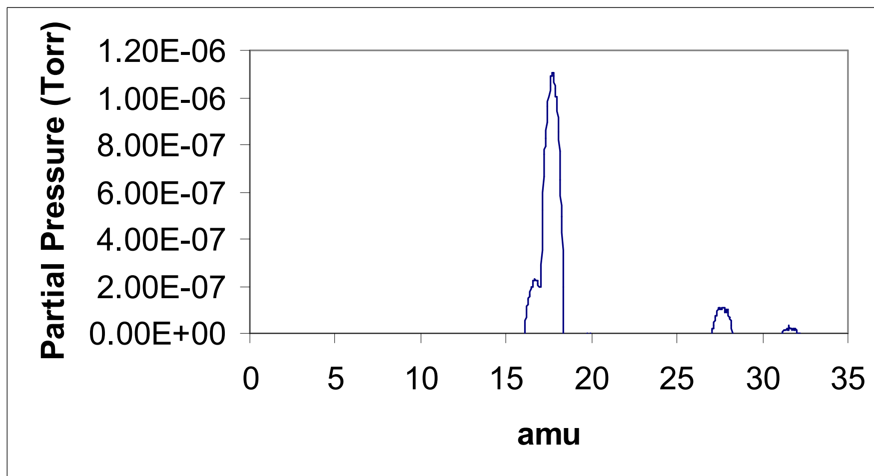

Figure 3.22. The mass spectra of B35 experiment before the process gases were given to the chamber (low partial pressure of nitrogen, peak located at 28 amu)

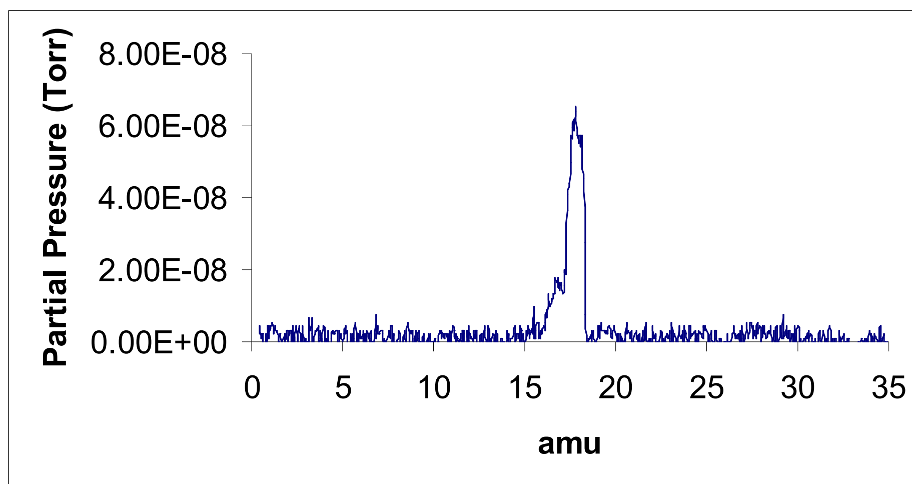

Figure 3.23. The mass spectra of B39 experiment before the process gases were given to the chamber (no partial pressure of nitrogen, peak located at 28 amu)

A typical mass spectra after the process gases were given to the system is shown in Figure 3.24. The peaks are diborane, nitrogen, argon and hydrogen and their peak locations are given in Table 3.16.

Typical mass spectrum after the plasma formation in the chamber are shown in figures 3.25 and 3.26. As seen from these spectrum, there was no diborane leaving the system as a residual gas since no peak could be seen in the range of 22 to 27 amu. The reason is considered to be that the diborane is highly reactive in this medium and dissociates into radicals and adsorbed on the substrates immediately.

To observe whether or not some heavy radicals were formed in the plasma medium, a wide range mass spectra was taken and given in Figure 3.26. It is clearly seen that no heavy radical formation occurred in the experiments.

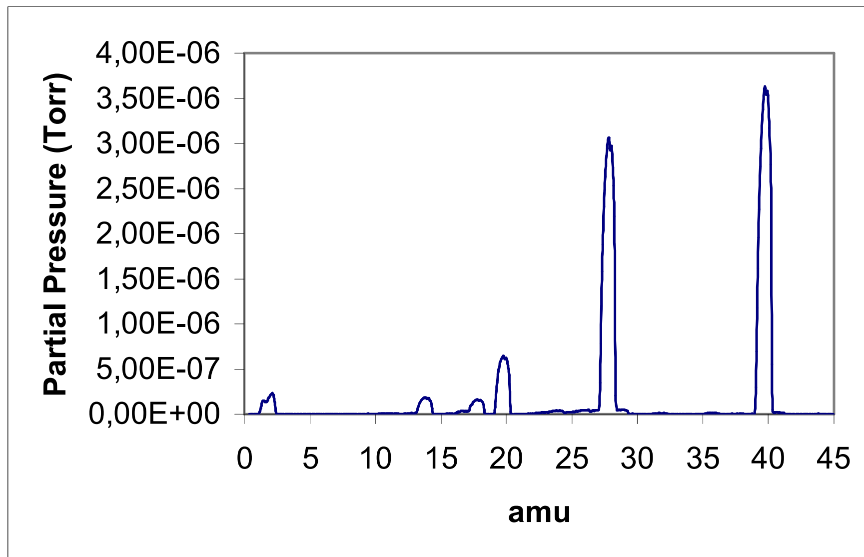

Figure 3.24. The mass spectra of B33 experiment after the process gases were given to the chamber

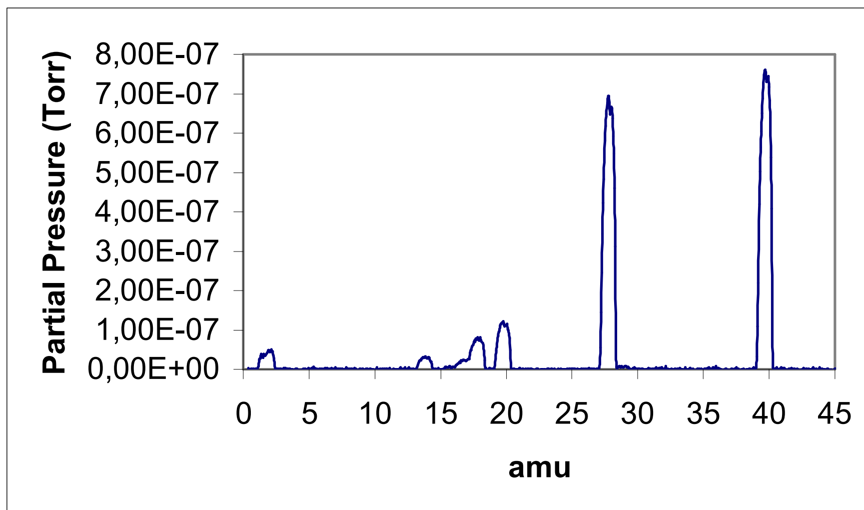

Figure 3.25. The mass spectra of B33 experiment after the plasma formation in the chamber

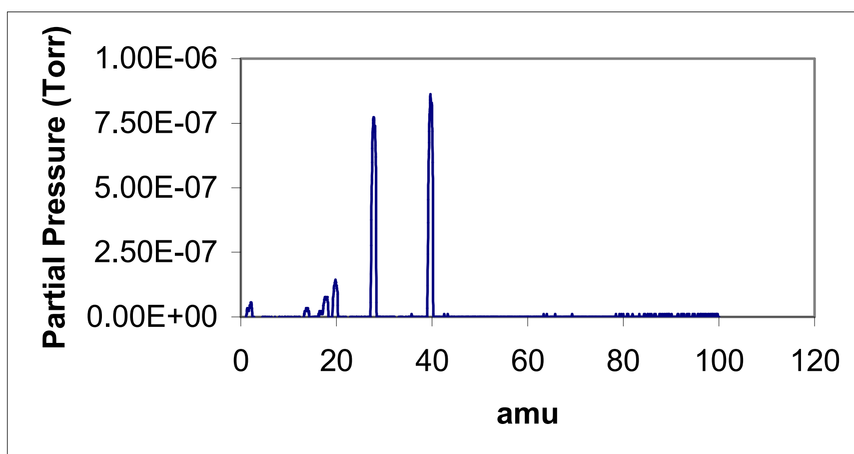

Figure 3.26. The wide mass spectra of B33 experiment after the plasma formation in the chamber

3.2.2.5. XPS Results

The surface atom concentrations of the films and the atom ratios on the surface are given in Table 3.17.

Table 3.17. The surface concentrations and the atom ratios of the films

Experiment	Surface Concentration (%)			Atom Ratio	
	B	N	O	N/B	O/B
B22	53.12	12.05	34.83	0.23	0.66
B23	64.43	11.24	24.33	0.17	0.38
B24	51.41	13.94	34.65	0.27	0.67
B25	62.65	8.90	28.44	0.14	0.45
B26	54.79	18.56	26.65	0.34	0.49
B33	56.37	7.51	36.13	0.13	0.64
B34	60.11	14.16	25.73	0.24	0.43
B35	96.01	0.00	3.99	0.00	0.04
B36	53.41	34.57	12.02	0.65	0.23
B38 Middle	61.83	3.33	34.84	0.05	0.56
B38 Edge	45.88	5.42	48.70	0.12	1.06

3.2.2.6. The Investigation of the Films Deposited By the Slave Unit of PECVD

Boron nitride thin films were deposited in the MW power generated reactor. Most of the deposited films were found to be in hexagonal form. Nevertheless, the onset of the cubic structure was also observed. The deposition rates of the deposited films in the slave unit of the PECVD system was found to be close to the films deposited with the master unit of the PECVD system. However, MW power assisted to have a more ordered structure, when the sharpnesses of the BN peaks were compared with the RF power assisted depositions.

3.2.2.6.1. The Effect of Pressure on the Deposited Films in the Slave Unit of the PECVD System

Decreasing the deposition pressure from 1 Torr to 0.1 Torr in B17 and B23 experiments has vanished the B-H and the N-H bond formation by increasing the ion energies in the plasma to etch weak hydrogen bonds, as seen in figures 3.12 and 3.13. Moreover, the broadening of the h-BN peak implies that the structure has more stress and it has increased the c-BN bonds slightly. Also, this broadening may be explained by the change of the crystal plane orientations. Nevertheless, although B28 experiment was carried out with 5 times diluted diborane, the high deposition rate was considered to be caused by the high pressure.

3.2.2.6.2. The Effect of Applied RF Power on the Deposited Films in the Slave Unit of the PECVD System

The addition of RF power to the system has eliminated the c-BN bond located at 1070 cm^{-1}, however; it has assisted to sharpen the transverse-optic (TO) h-BN peak located at 1380 cm^{-1} as seen in figures 3.13 and 3.14. Although, it has no effect on forbidden energy band-gaps, it has decreased the film deposition rates as given in tables 3.14 and 3.15. As a result, it may be considered that the increased ion energies with addition of RF power have etched the weak bonds in depositing layers, so decreased the deposition rate. On the other hand, as seen from the IR spectrum, a

better h-BN structure was observed, in terms of stability and crystallinity. The adhesion of the films lasted longer and from the IR spectrum, the BN crystals were more oriented in the parallel direction to the substrates, which was understood from the sharpness of the BN peaks.

3.2.2.6.3. The Effect of N_2/B_2H_6 Gas Ratio on the Deposited Films in the Slave Unit of the PECVD System

It is seen from the XPS results that the film surfaces contain about 50% boron and from the residual gas analysis boron is found to be so reactive. Therefore it seems that the N_2/B_2H_6 ratio in the gas mixture must kept as high as possible to have N/B ratio on the surface close to 1. For this purpose, the gas ratio was increased from 10 to 25, then to 50 and lastly to 100 as seen in Figure 3.16. This increase has led to an increase in the forbidden energy band-gaps in the films, however; it has increased the peak located at 1270 cm^{-1} and decreased the TO h-BN peak located at 1380 cm^{-1}. So, an undesired structure that is most probably boron-rich amorphous BN [34] in the film arose with increasing N_2/B_2H_6 gas ratio in MW PECVD system.

3.2.2.6.4. The Effect of Applied Bias Voltage on the Deposited Films in the Slave Unit of the PECVD System

It can be concluded from Figure 3.18 that the applied voltage led to better adhesion of the films. For 15 days, no structural change was observed. So it has a positive effect on the stability of the deposited films.

3.2.2.6.5. The Effect of Addition of Argon Gas to the Process Gases on the Deposited Films in the Slave Unit of the PECVD System

Addition of argon gas to the process gases has broadened the h-BN peaks as seen in figures 3.14 and 3.15. The reason for this broadening is considered to be the change of the crystal plane directions in the film. Since the TO h-BN peak was decreased, the planes were less parallel oriented to the substrate. Due to this change, an increase

in the film stress may be expected. Argon was considered to etch the weak bonds in the film, so the forbidden energy band-gap was increased due to larger crystalline islands in amorphous matrix. On the other hand, since argon gas acts as an etchant in the deposition process, the content of argon in the reaction gas mixture should be optimized.

3.2. THE ANALYSES OF THE FILMS DEPOSITED IN SPUTTERING SYSTEM

For the deposition of the boron nitride films in sputtering system, hexagonal boron nitride target was subjected to energetic ion bombardment. Double side polished silicon, glass and quartz were used as substrates. The deposition parameters of the sputtering system are given in Table 3.18.

Table 3.18. The deposition parameters for the sputtering system

Experiment	RF Power (W)	Pressure (mbar)
B44	300	2
B45	400	2
B46	550	2
B47	550	1
B50	800	3

3.2.1. FTIR Results

For the characteristic IR absorptions of the films deposited by sputtering, B46 and B50 experiments are given in Figure 3.27.

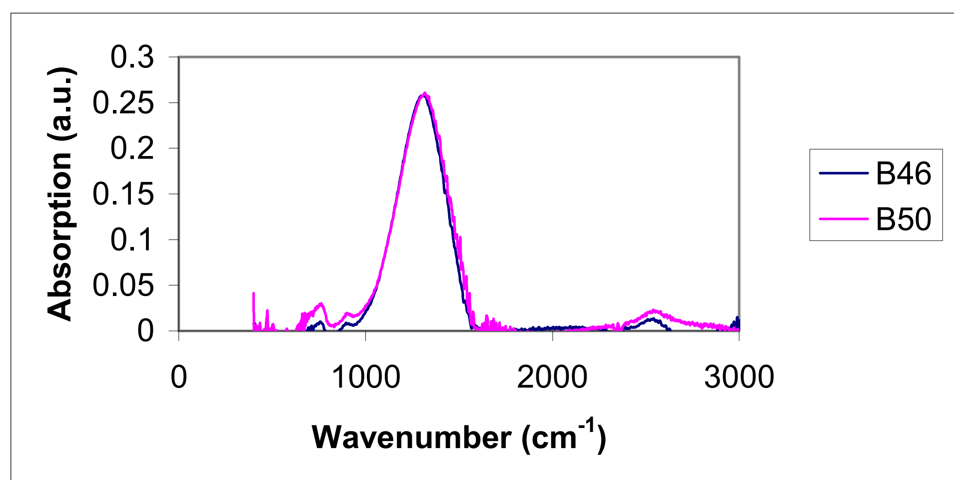

Figure 3.27. The IR spectrum of B46 and B50 experiments

Although only argon gas was used during the deposition process, still B-H peak located at 2500 cm^{-1} was observed in the IR spectrum. This B-H structure was considered to be due to the adsorption of water vapor from the atmosphere. The orientatiton of the crystal planes did not change neither with the power increase, nor with the deposition pressure increase.

3.2.2. UV-Vis Results

A typical UV-Vis spectra for sputtering deposited films was B49 experiment and it is shown in Figure 3.28.

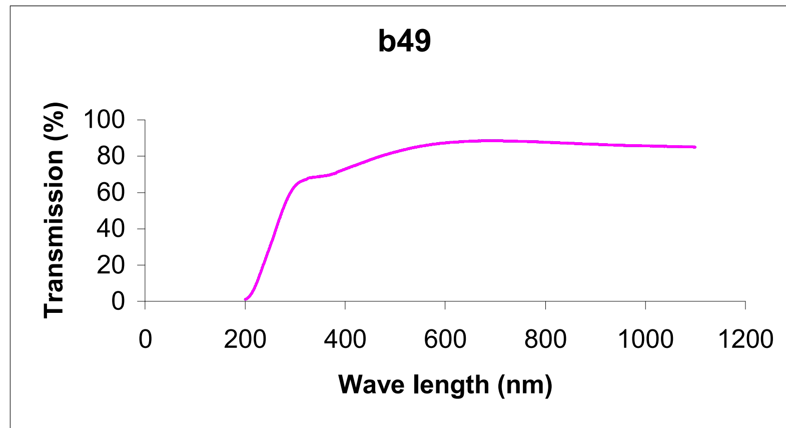

Figure 3.28. The UV-Vis spectra of the B49 experiment

For the determination of the forbidden energy band-gaps, absorption coefficients of the films were calculated by using Eqn. 3.1.

For the normalization with thickness, all films that could not be measured were assumed to be 100nm thick. The energy corresponding to the α of 10^4 cm^{-1} was taken as a measure of the forbidden band-gap and results are tabulated in Table 3.19.

Table 3.19. The forbidden band-gaps of the experiments

Experiment	Forbidden Band-Gap (eV)
B45	2.15
B48	1.39
B49	2.44
B50	2.35

3.2.3. Profilometer Results

The thicknesses determined by profilometry and the deposition rates of the films deposited by sputtering are given in Table 3.20.

Table 3.20. The thicknesses and the deposition rates of the films

Experiments	Thickness (nm)	Deposition Rate (nm/min)
B44	70	1.75
B45	100	0.76
B46	125	1.17
B47	300	3.75
B50	110	1.96

3.2.4. The Investigation of the Films Deposited By the Sputtering System

Boron nitride thin films were deposited in sputtering system. The deposited films were found to be hexagonal. The observed film deposition rates were slow when compared to the other deposition systems.

3.2.4.1. The Effect of Pressure on the Deposited Films in the Sputtering System

Pressure was continuously changed during B48 and B49 experiments. The effect of pressure to the film thickness was followed by XTC monitor. Reducing the deposition pressure from 3 to 2 mbar at 550 W led to an increase in the film deposition rate from 2.8 to 3.2 nm/min. The same effect could be seen for B46 and B47 experiments in Table 3.20. As seen in Figure 3.27, the deposition pressure had no effect on the structure of the films, since the h-BN peak showed no difference.

3.2.4.2. The Effect of the Applied RF Power on the Deposited Films in the Sputtering System

The applied RF power was continuously changed during B48 and B49 experiments. The effect of the applied RF power to the film thickness was followed by XTC monitor. Increasing the power from 550W to 600W at 2 mbar led to an increase in the film deposition rate from 3.2 to 3.7 nm/min by increasing the energies of the sputtering ions. The same effect could be seen for B45 and B46 experiments in Table 3.20. As seen in Figure 3.27, the applied RF power had no effect on the structure of the films, since the h-BN peak located at 1380 cm^{-1} showed no difference.

CHAPTER 4

CONCLUSIONS AND RECOMMENDATIONS

Boron nitride thin films were deposited on silicon, quartz and glass substrates in both units of the PECVD system and in the sputtering system. Most of the deposited films were determined to be in hexagonal structure; however, the cubic onset has been observed in some of the films. While depositing the films, bias voltage applied to the substrates, substrate temperature, deposition pressure, N_2/B_2H_6 process gas ratios and addition of argon gas to the process gases, and the applied RF and/or MW power were varied in each experiment. The effects of these parameters were investigated by FTIR spectroscopy for structural changes, UV-Vis spectroscopy for energy band-gap changes and profiometry for the film thicknesses and deposition rate changes. The atom concentrations on the film surfaces were determined by XPS analysis, which was carried out at the Central Laboratory. Residual gas analysis was carried out by mass spectrometer.

It was observed that the reducing the pressure led to an increase in the BN content of the films by eliminating the N-H and B-H bond formation. Moreover using MW power at low pressures led to the c-BN formation. However, the deposition rates of the films were decreased with reducing the pressure in the PECVD system. On the other hand, decreasing the deposition pressure in the sputtering system led to an increase in the deposition rates. So, to increase the BN content, pressure should be as low as possible.

Increase in applied RF power in both sputtering system and the master unit of the PECVD led to an significant increase on the deposition rates. However, it did not effect the structure of the films. On the other hand, when RF power was added to the MW power, the c-BN peak in the IR spectra vanished but the h-BN peak got

narrower. More crystalline and stable h-BN films were observed by using both kinds of power supplies at the same time.

Applying negative bias voltage on the substrates had increased both the number of the BN bonds and the forbidden band-gaps of the films. Although it has no effect on the structure of the films or the deposition rates, it was considered to lead to better adhesion of the films.

Increasing the substrate temperature in the master unit of the PECVD system showed positive effects on the h-BN films. First of all, with increasing the temperature N-H and B-H bonds were decreased, so hydrogen contamination decreased. Secondly the mechanical and chemical stability of the films and the adhesion on the substrates got better. The h-BN crystallinity and the forbidden band-gaps were increased. Although the deposition rate has decreased with increasing the substrate temperature, it should be kept as high as possible for better BN films.

The N_2/B_2H_6 gas ratio was considered to be kept as high as possible for the unity of the N/B ratio on the surface. Although the gas ratio was increased to 100, no significant change in the N/B ratio on the surface could be observed. However, it had increased the forbidden energy band-gaps significantly. Moreover, the undesired amorphous BN structure in the films were increased with increasing this gas ratio.

Addition of the argon gas to the gas mixture led to the broadening of the h-BN peak in the IR spectrum. Since argon acts as an etchant, the argon amount in the gas mixture should be optimized.

Cubic structure could be observed only when the MW power was used. h-BN films were succesfully deposited in both PECVD and sputtering systems. The deposition rates of the master and the slave unit of the PECVD were determined to be close to each other, whereas the deposition rates obtained by sputtering were so low when compared to the PECVD. In literature, no c-BN formation occured without applying bias voltage to the substrates as seen from Table 1.4. Moreover, it was shown that temperature has positive effects on cubic structure formation [15]. Therefore a

voltage supply and a substrate heater should be adapted to the sputtering system for further studies.

For safety issues, instead of using toxic gases in PECVD system, sputtering system should be preferred. Because only argon, or additionally nitrogen as reported in the literature [17-22] were used to sputter the h-BN target.

The parameters were surveyed in the literature for both PECVD and sputtering systems and given with the covered areas during the experiments in tables 4.1 and 4.2, respectively. It is thought that future study in the uncovered areas will be beneficial for the production of BN with cubic structure.

Table 4.1. The literature limits and covered values in experiments for PECVD system

Parameters	Min	Covered	Max
RF Power (W)	200	200 - 270	500
MW Power (W)	200	800	1400
Substrate Temperature (°C)	200	23 - 350	900
Negative Bias Voltage (V)	0	0 - 250	160
Deposition Pressure (mTorr)	1.6	100 - 500	1000

Different boron and nitrogen precursors were used for CVD routes in the literature as seen in Table 1.3. The gases, such as BF_3 and BCl_3 could be used as boron sources and these precursors may have positive effect on the cubic structure formation.

Table 4.2. The literature limits and covered values in experiments for sputtering system

Parameters	Min	Covered	Max
Magnetron Power (W)	60	300-800	800
Deposition Pressure (mbar)	1.3×10^{-3}	1-7	30
Substrate Temperature (°C)	27	-	600
Negative Bias Voltage (V)	50	-	300

REFERENCES

[1] Anutgan M., 'Investigation of Plasma Deposited Hexagonal Boron Nitride Thin Films', *M.S. Thesis, Physics Department*, *Middle East Technical University*, *2007*

[2] P.B. Mirkarimi, K.F. McCarty, D.L. Meldin, *Materials Science and Engineering*, **R21** (1997), 47-100

[3] Bor Raporu, www.kimyamuhendisi.org

[4] I. Bello, Y.M. Chong, K.M. Leung, C.Y. Chan, K.L. Ma, W.J. Zhang, S.T. Lee, A. Layyous, *Diamond and Related Materials*, **14** (2005), 1784-1790

[5] M. Kuhr, S. Reinke, W. Kulisch, *Diamond and Related Materials*, **4** (1995), 375-380

[6] J.R. Roth, Industrial Plasma Engineering, Vol. 1, IOP Publishing, Midsomer Norton, Somerset, 2000

[7] A. Anders, Handbook of Plasma Immersion Ion Implantation and Deposition, john Wiley & Sons, Inc., USA, 2000

[8] M.N.P. Carreno, J.P. Bottecchia, I. Pereyra, *Thin Solid Films*, **308–309** (1997), 219–222

[9] A. Abdellaoui, A. Bath, B. Bouchikhi, O. Baehr, *Materials Science and Engineering*, **B47** (1997), 257-262

[10] M. Ben el Mekki, N.Mestres, J. Pascual, M.C. Polo, J.L. Andujar, *Diamond and Related Materials*, **8** (1999), 398–401

[11] F. Rossi, C. Schaffnit, L. Thomas, H. del Puppoa, R. Hugon, *Vacuum*, **52** (1999), 169-181

[12] J. Vilcarromero, M.N.P. Carreno, I. Pereyra, *Thin Solid Films*, **373** (2000), 273-276

[13] A. Soltani, P.Thevenin, A.Bath, *Diamond and Related Materials*, **10**(2001), 1369-1374

[14] B. Deb, B. Bhattacharjee, A. Ganguli, S. Chaudhuri, A.K. Pal, *Materials Chemistry and Physics*, **76** (2002), 130–136

[15] C.Y. Chan, W.J. Zhang, X.M. Meng, K.M. Chan, I. Bello, Y. Lifshitz, S.T. Lee, *Diamond and Related Materials*, **12** (2003), 1162–1168

[16] G.A. Battiston, D. Berto, A. Convertino, D. Emiliani, A. Figueras, R. Gerbasi, S. Viticoli, *Electrochimica Acta*, **50** (2005), 4600–4604

[17] S. Ulrich, H. Ehrhardt, J. Schwan, W. Donner, H. Dosch, P. Widmayer, P. Ziemann, *Surface and Coatings Technology,* **116–119** (1999), 269–273

[18] Z.F. Zhou, I. Bello, V. Kremnican, M.K. Fung, K.H. Lai, K.Y. Li, C.S. Lee, S.T. Lee, *Thin Solid Films*, **368** (2000), 292-296

[19] L. Jiang, A. G. Fitzgerald, M. J. Rose, A. Lousa, S. Gimeno, *Surf. Interface Anal.,* **34 (**2002), 732–734

[20] X.Z. Ding, X.T. Zeng, H. Xie, *Thin Solid Films*, **429** (2003), 22–27

[21] S. Kotake, T. Hasegawa, K. Kamiya, Y. Suzuki, T. Masui, Y. Kangawa, K. Nakamura, T. Ito, *Applied Surface Science*, **216** (2003), 72–77

[22] Y.K. Le, H. Oechsner, *Thin Solid Films*, **437** (2003), 83–88

[23] J. M. Caicedo, G. Bejarano, G. Zambrano, E. Baca, O. Moran, P. Prieto, *Phys. Stat. Sol. (b)*, **242, No. 9** (2005), 1920–1923

[24] Atılgan I., ‘The Production and Characterization of Si Thin Films’, *Ph.D Thesis*, *Physics Department*, *Middle East Technical University*, *1993*

[25] Sel K., ‘The Effects of Carbon Content on the Properties of Plasma Deposited Amorphous Silicon Carbide Thin Films’, *Ph.D Thesis*, *Physics Department*, *Middle East Technical University*, *2007*

[26] User Manual

[27] J.W. Niemantsverdriet, Spectroscopy in Catalysis, Wiley-VCH, Darmstadt, 2000

[28] Postole G., Caldararu M., Ionescu N.I., Bonnetot B., Auroux A., Guimon C., *Boron nitride: A high potential support for combustion catalysts*, Thermochimica Acta 434, 2005, pp. 150–157

[29] Franz,D., Hollenstein,M., Hollenstein, C., 2000, *Diborane nitrogen ammonia plasma chemistry investigated by infrared absorption spectroscopy*, Thin Solid Films 379_2000.37]44

[30] Gomez-Aleixandre,C.,Essafti, A., Fernandez, M.,Fierro,J.L.G.,Albella,J.M., 1996, *Influence of Diborane Flow Rate on the Structure and Stability of CVD Boron Nitride Films*, *J. Phys. Chem.* 1996, *100,* 2148-2153

[31] Andujar,J.L.,Bertran,E.,Polo, M.C., 1998, *Plasma-enhanced chemical vapor deposition of boron nitride thin films from B_2H_6–H_2–NH_3 and B_2H_6–N_2 gas mixtures*, J. Vac. Sci. Technol. A 16.2., Mar/Apr 1998

[32]Battiston,G.A.,Berto,D.,Convertino,A.,Emiliani,D.,Figueras,A.,Gerbasi,R.,Viticoli,S.,2005, *PECVD of h-BN and c-BN films from boranedimethylamine as a single source precursor*, Electrochimica Acta 50 (2005) 4600–4604

[33] P.B. Mirkarimi, K.F. McCarty, D.L. Meldin, 1997, *Review of advances in cubic boron nitride film synthesis*, Mat. Sci. & Eng. R21 (1997) 47-100

[34] J. Tian, L. Xia, H. Zhang, S. Lee, F. Lu, W. Tang, 2001, *Effect of nitrogen ion implantation on the microstructural transformation of boron film*, Thin Solid Films 401 (2001) 106–110

[35] A. Olszyna, J. Konwerska-Hrabowska, M. Lisicki, 1997, Molecular structure of E-BN, Diamond and Related Materials 6 (1997) 617-620

[36] J.B. Wang, G.W. Yang, C.Y. Zhang, X.L. Zhong, ZH.A. Ren, 2003, *Cubic-BN nanocrystals synthesis by pulsed laser induced liquid–solid interfacial reaction*, Chemical Physics Letters 367 (2003) 10–14

[37] H.S. Kim, I.H. Choi, Y.-J.Baik, Surf. Coat. Technol. 133-134, 2000, 473-477